

UNRAVELING CORAL NUTRITION STRATEGIES IN RESPONSE TO  
NUISANCE MACROALGAE: INSIGHTS FROM AMINO ACID ISOTOPIC  
ANALYSIS IN THE NORTHWESTERN HAWAIIAN ISLANDS

A THESIS SUBMITTED TO THE GRADUATE DIVISION OF  
THE UNIVERSITY OF HAWAI'I AT MĀNOA IN PARTIAL  
FULFILLMENT OF THE REQUIREMENTS FOR THE  
DEGREE OF

MASTER OF SCIENCE

IN

OCEANOGRAPHY

JUNE 2024

By Mario Kaluhiokalani

Thesis Committee:  
Brian Popp, Chairperson  
Andrea Kealoha  
Craig Nelson  
Christopher Wall

Keywords: Coral, isotopes, *Chondria tumulosa*,  
Northwestern Hawaiian Islands

## **ACKNOWLEDGMENTS**

I would like to acknowledge and thank my thesis committee namely Dr. Brian Popp and Dr. Chris Wall. Their dedication to my success was unrelenting and I am very grateful for their mentorship and support. I would also like to thank members Dr. Andrea Kealoha and Dr. Craig Nelson for their wisdom and input to make my work strong and effective. I am grateful to have been afforded an opportunity to pursue research in a part of the world that few people get to see and experience.

To the labs and people that call them home! Ford, Kira, and Josh from the Coral Resilience Lab helped me get my start in science and have supported me unconditionally. To Natalie Wallsgrove, your ability to stay on top of things while demonstrating help and patience is a real inspiration. Absolutely instrumental in the Popp Lab! To Bradda Cliff, JB, and Kailey out of the MEGA Lab! True legends of bridging science and culture acting as an accelerant to the spark of my scientific passion.

Furthermore, I would like to dedicate this work to Jocelyn Kellogg. A woman who has raised one of my best friends and has gone too soon. Your determination and positive energy was absolutely prolific.

I would like to acknowledge and thank my Mom, Julie, and all of the strong women that have raised me. I am eternally grateful for your love and support. To my wahine, Makena, I am thankful for your unwavering dedication and patience. And to my friends near and far who have been rooting for me all this time. Mahalo nui loa!

## ABSTRACT

Coral reef ecosystems are under increasing threat from local and global stressors, including the introduction and proliferation of invasive species. Understanding coral nutrition strategies in response to environmental stress is crucial for predicting reef resilience. This study investigates the impact of macroalgal cover, specifically the nuisance red alga *Chondria tumulosa*, on nutritional strategies of two corals (*Montipora capitata*, *Pocillopora* spp.) in the Northwestern Hawaiian Islands (NWHI). Coral samples were collected pre- and post-invasion of *C. tumulosa*, with bulk tissue and compound-specific isotopic analysis of amino acids (CSIA-AA) employed to assess coral nutrition. Bulk carbon and nitrogen stable isotopic compositions ( $\delta^{13}\text{C}$ ,  $\delta^{15}\text{N}$ ) revealed coupled nutritional reliance between coral host and symbiont with a consistent  $\delta^{13}\text{C}$  decrease with depth. CSIA-AA demonstrated significant separation in essential amino acid  $\delta^{13}\text{C}$  fingerprints between coral hosts, symbionts, plankton, and *C. tumulosa* relating to autotrophic fidelity in *M. capitata* and trophic plasticity in *Pocillopora* consistent with previous work. Trophic position ( $\text{TP}_{\text{Glx-Phe}}$ ) of plankton was  $2.3 \pm 0.6$ , consistent with primary consumers, while coral  $\text{TP}_{\text{Glx-Phe}}$  indicate high reliance on autotrophy in *M. capitata* ( $\text{TP}_{\text{Glx-Phe}}$ :  $1.1 \pm 0.2$ ) and greater heterotrophic feeding on plankton in *Pocillopora* spp. ( $\text{TP}_{\text{Glx-Phe}}$ :  $1.6 \pm 0.4$ ). A higher-than-expected  $\text{TP}_{\text{Glx-Phe}}$  was found in *C. tumulosa* ( $1.5 \pm 0.1$ ), suggesting inclusion of heterotrophic bacteria living on or among the macroalgae. It is unlikely that *Pocillopora* spp. obtained nutrition directly from *C. tumulosa*, however, our work suggests that essential amino acid  $\delta^{13}\text{C}$  values can be used to identify organisms that prey on *C. tumulosa*. These findings underscore the importance of understanding coral-algal interactions in the face of environmental change and highlight the utility of CSIA-AA in elucidating complex trophic dynamics within coral reef ecosystems.

# TABLE OF CONTENTS

<b>ACKNOWLEDGMENTS</b> .....	<b>i</b>
<b>ABSTRACT</b> .....	<b>ii</b>
<b>LIST OF TABLES</b> .....	<b>iv</b>
<b>LIST OF FIGURES</b> .....	<b>v</b>
<b>INTRODUCTION</b> .....	<b>7</b>
<b>METHODS</b> .....	<b>13</b>
Sample Collection .....	13
Laboratory Analysis .....	13
Bulk tissue stable isotope analysis .....	13
Individual amino acid isotope analysis .....	14
Data Analysis .....	15
<b>RESULTS</b> .....	<b>18</b>
Bulk isotopes .....	18
$\delta^{13}\text{C}$ AA analysis .....	18
Linear discriminant analysis .....	19
<i>Chondria tumulosa</i> effect .....	20
$\delta^{15}\text{N}$ AA analysis .....	20
Amino acid trophic position .....	21
<b>DISCUSSION</b> .....	<b>22</b>
<b>CONCLUSION</b> .....	<b>27</b>
<b>SUPPLEMENTAL MATERIAL</b> .....	<b>43</b>
<b>REFERENCES CITED</b> .....	<b>53</b>

## LIST OF TABLES

<b>Table 1.</b> Results of PERMANOVA testing effects of tissue fraction†, genus, site, and <i>C. tumulosa</i> abundance* on amino acid carbon and nitrogen isotope values .....	28
<b>Table 2.</b> Results of pairwise PERMANOVA testing the effect of tissue fraction interactions on amino acid carbon isotope values. ....	29
<b>Table 3.</b> PERMANOVA results comparing $\delta^{13}\text{C}_{\text{EAA}}$ to the % <i>C. tumulosa</i> coverage. % <i>C. tumulosa</i> coverage binned into none, low, moderate, and high abundance. ....	30
<b>Table 4.</b> ANOVA results of individual EAA $\delta^{13}\text{C}$ values comparing the effect of % <i>C. tumulosa</i> on pooled host samples. ....	31
<b>Table 5.</b> PERMANOVAs of mean-normalized $\delta^{13}\text{C}_{\text{EAA}}$ values between like tissue types of samples comparing this study's data to previous literature .....	32
<b>Table S1.</b> Sample collection/analysis metadata link.....	43
<b>Table S2.</b> ANOVA tests of mean-normalized essential amino acid $\delta^{13}\text{C}$ values between coral hosts, symbionts, plankton, and <i>C. tumulosa</i> .....	44
<b>Table S3.</b> Individual ANOVA results comparing <i>Montipora</i> and <i>Pocillopora</i> essential amino acid $\delta^{13}\text{C}$ values. ....	45
<b>Table S4.</b> Results of linear discriminant analysis comparing EAA of genera: <i>Montipora</i> , <i>Pocillopora</i> , Symbionts, Plankton, and <i>C. tumulosa</i> . ....	46
<b>Table S5.</b> Pairwise PERMANOVAs of $\delta^{15}\text{N}$ values between fractions.....	47
<b>Table S6.</b> Pairwise PERMANOVAs of $\delta^{15}\text{N}$ values between genera .....	48

## LIST OF FIGURES

<b>Fig. 1.</b> Bulk $\delta^{13}\text{C}$ and $\delta^{15}\text{N}$ values of <i>Montipora</i> and <i>Pocillopora</i> coral host and symbiont tissue. ....	33
<b>Fig. 2.</b> Bulk $\delta^{13}\text{C}$ values with depth (m) between <i>Montipora</i> and <i>Pocillopora</i> coral hosts and symbionts..	34
<b>Fig. 3.</b> Bulk host $\delta^{13}\text{C}$ values minus $\delta^{13}\text{C}$ symbiont values for <i>Montipora</i> and <i>Pocillopora</i> relative to depth (m) of the colony sampled.....	35
<b>Fig. 4.</b> Bulk $\delta^{13}\text{C}_{\text{H-S}}$ values as a function of varying % <i>C. tumulosa</i> cover. ....	36
<b>Fig. 5.</b> Mean-normalized $\delta^{13}\text{C}$ values of essential amino acids between pooled coral hosts, pooled symbionts, plankton, and <i>C. tumulosa</i> . ....	37
<b>Fig. 6.</b> Principal component analysis from $\delta^{13}\text{C}_{\text{EAA}}$ values of corals: <i>Montipora capitata</i> & <i>Pocillopora</i> spp., symbionts, plankton, and <i>C. tumulosa</i> . ....	38
<b>Fig. 7.</b> Linear discriminant analysis of $\delta^{13}\text{C}_{\text{EAA}}$ for <i>Montipora</i> and <i>Pocillopora</i> corals, symbiont and zooplankton endmembers with <i>C. tumulosa</i> included .....	39
<b>Fig. 8.</b> Boxplot of host $\delta^{13}\text{C}_{\text{EAA}}$ values of each AA under various % <i>C. tumulosa</i> coverage binned into none, low, moderate, and high.....	40
<b>Fig. 9.</b> $\delta^{15}\text{N}_{\text{AA}}$ values of Trophic and Source * AA for <i>Montipora</i> and <i>Pocillopora</i> corals, plankton, and <i>C. tumulosa</i> .....	41
<b>Fig. 10.</b> Boxplot of trophic position ( $\text{TP}_{\text{Glx-Phe}}$ ) of groups: <i>Montipora</i> , <i>Pocillopora</i> , plankton and <i>C. tumulosa</i> .....	42
<b>Fig. S1.</b> $\delta^{15}\text{N}_{\text{H-S}}$ values of <i>M. capitata</i> and <i>Pocillopora</i> spp. corals over a depth gradient between years 2015, 2021, and 2022 .....	49
<b>Fig. S2.</b> Bulk $\delta^{15}\text{N}$ host minus symbiont values as a function of varying % <i>C. tumulosa</i> cover for <i>M. capitata</i> and <i>Pocillopora</i> spp. corals. ....	50
<b>Fig. S3.</b> Raw amino acid $\delta^{13}\text{C}$ values found from CSIA-AA of <i>M. capitata</i> , <i>Pocillopora</i> spp., pooled symbionts, plankton, and <i>C. tumulosa</i> . ....	51
<b>Fig. S4.</b> PCA of $\delta^{13}\text{C}_{\text{EAA}}$ values of Chondria compared to other genera of Pacific red algae reported by Elliott Smith (2022).....	52

## LIST OF ABBREVIATIONS

AA	Amino Acid
Ala	Alanine
ANCOVA	Analysis of Co-variance
ANOVA	Analysis of Variance
Asp	Aspartic Acid
C	Carbon
CSIA-AA	Compound-Specific Isotope Analysis of Amino Acids
EAA	Essential Amino Acids
GC-C-IRMS	Gas Chromatography Combustion Isotope Ratio Mass Spectrometry
Glx	Glutamic Acid
Gly	Glycine
Ile	Isoleucine
IRMS	Isotope Ratio Mass Spectrometer
LDA	Linear Discriminant Analysis
Leu	Leucine
Lys	Lysine
N	Nitrogen
NEAA	Non-Essential Amino Acids
NWHI	Northwestern Hawaiian Islands
PCA	Principal Component Analysis
PERMANOVA	Permutational Multivariate Analysis of Variance
POM	Particulate Organic Matter
Pro	Proline
Phe	Phenylalanine
Ser	Serine
TDF	Trophic Discrimination Factor
Thr	Threonine
TP <sub>Glx/Phe</sub>	Trophic Position
Tyr	Tyrosine
Val	Valine
V-PDB	Vienna Pee-Dee Belemnite
δ	Delta Isotope Analysis

## INTRODUCTION

Scleractinian reef-building corals are the engineers of coral reefs and exist as mixotrophic organisms, composed of a polyp animal and a community of photosynthetic dinoflagellates (Symbiodiniaceae; LaJeunesse et al 2020) and microbes, collectively called the coral holobiont (Aprill 2020). In oligotrophic tropical seas, nutritional exchanges in the coral-Symbiodiniaceae symbiosis form the foundation of coral reef food webs. The coral animal receives symbiont-derived photosynthates and amino acids from Symbiodiniaceae that support coral growth and nutrition (Wang and Douglas 1998), and in return, the symbiont community receives host metabolic waste that supports algae growth (Morris et al. 2019). In addition to symbiont photosynthates as a source of autotrophic nutrition, the coral host possesses a diverse capacity for heterotrophic feeding, consuming an array of zooplankton, bacteria, and particulate organic matter (POM) in the water column (Houlbrèque and Ferrier-Pagès, 2009, Mills and Sebens, 2004).

It is generally accepted that the symbiotic algae within the host cell can provide up to 95% of the coral's energy demand (Muscatine et al. 1981). However, the ratio of autotrophy to heterotrophy varies between coral species, environmental conditions, and in response to environmental stress (Wall et al. 2019, Palardy et al. 2005, Fox et al. 2018). Stressful environmental conditions like increased sea surface temperature can lead to coral bleaching – a dysbiosis in which corals expel their algal symbionts, causing the coral tissue to turn pale or white in color (Glynn 1984). Without these symbionts, corals can become weakened and more susceptible to disease, predation, and other stressors (Burge et al., 2014).

Disruptions to autotrophic nutrition – such as those caused by bleaching events, environmental stressors, or depth-dependent light attenuation – can result in increased coral reliance on heterotrophic nutrition and a greater proportion of heterotrophically-derived carbon in coral energy budgets (Grottoli 2006, Palardy et al. 2008, Levas et al. 2013). Research has also suggested that corals that rely more on heterotrophic nutrition may be better equipped to resist bleaching and survive post-bleaching stress (Conti-Jerpe et al. 2020).

Coral nutrition can be assayed using a variety of methods, including respirometry to measure photosynthetic rates and feeding trials where zooplankton are provided to corals *ad libitum* (Grottoli, 2006). In a 2006 lab experiment, the feeding rates of bleached and non-bleached *Montipora capitata* and *Porites compressa* were calculated, and results suggested corals modify their trophic strategy to meet energy needs (i.e., trophic plasticity), either by consuming energy reserves or by increasing heterotrophic nutrition in the form of zooplanktivory (Grottoli 2006). In the absence of zooxanthellae, *M. capitata* were able to fully transition to heterotrophic feeding, whereas *P. compressa* maintained natural feeding rates and relied on energy reserves and biomass to make up for the photosynthetic deficit (Grottoli 2006). This study and its experimental approach has resulted in renewed interest in the role of species-specific capacities for heterotrophy in coral energy budgets, as well as the influence of trophic plasticity in shaping coral physiological resilience in the face of local and global environmental challenges (ocean acidification, thermal bleaching, nutrient pollution) (Wall et al. 2019, Palardy et al. 2005, Fox et al. 2018). While the aforementioned measurements provide immediate estimates of production and predation, they do not provide time-integrated measurements of organism nutrition. Carbon (C) and nitrogen (N) stable isotope analysis ( $\delta^{13}\text{C}$  and  $\delta^{15}\text{N}$  values) of coral symbionts and host tissue provides insights into metabolic processes (Ferrier-Pagès and Leal, 2019).

Carbon is assimilated by the holobiont from both autotrophic and heterotrophic sources with a distinct range of  $\delta^{13}\text{C}$  values.  $\delta^{13}\text{C}$  values are frequently utilized in coral studies to discern the proportion of  $^{13}\text{C}$ -depleted heterotrophic prey compared to  $^{13}\text{C}$ -enriched autotrophic photosynthates (Muscatine et al. 1989; Laws et al. 1997). Following this approach, lower  $\delta^{13}\text{C}$  values in the host, or host values compared to those measured in the symbionts (referred to as host–symbiont  $\delta^{13}\text{C}$  values or  $\delta^{13}\text{C}_{\text{H-S}}$ ), are indicative of a higher dependence on heterotrophic nutrition (Rodrigues and Grottoli, 2006). This assay was also proven to work for  $\delta^{15}\text{N}$  values between hosts and symbionts ( $\delta^{15}\text{N}_{\text{H-S}}$ ) in determining trophic strategy (Conti-Jerpe et al. 2020) as  $\delta^{15}\text{N}$  values are known to increase in consumers relative to prey items ( $\sim 3.5$  per mill ‰), (DeNiro & Epstein 1981, Post 2002). As such, analyzing the  $\delta^{13}\text{C}$  and  $\delta^{15}\text{N}$  values of coral host tissue and symbionts separately can enhance our understanding of coral physiology, trophic ecology, and the degree of heterotrophic nutrition (Fox et al. 2019, Lesser et al., 2022). A recent study used  $\delta^{13}\text{C}$  and  $\delta^{15}\text{N}$

values of symbionts and *M. capitata* and *P. compressa* host tissues to discern differences in physiology from bleached and unbleached corals in Hawai'i conducted during and after a marine heatwave across shallow reef habitats. Wall et al. (2019) concluded that the composition (lipid content) and catabolism of coral host biomass supported coral metabolism during bleaching and recovery, with limited evidence for increased heterotrophic feeding. Therefore, while it is expected that some corals will exhibit trophic plasticity, able to acquire nutrients from multiple sources, others will demonstrate autotrophic fidelity, relying completely on nutrients from the photosynthetic symbiont. It is noted that the success of a particular coral species in a given environment may depend on both the composition and catabolism of its host biomass and its ability to acclimate to shifting resource landscapes (Fox et al. 2018, Wall et al., 2021). Bulk isotope analysis has been used for decades to study dietary preferences in complex systems (Boecklen et al. 2011), however, the assay is limited when evaluating highly complex and variable nutrient sources and internal nutrient recycling in corals (Post 2002, Chikaraishi et al. 2009, Radecker et al. 2015, Williams et al. 2018).

Recently, analysis of the carbon and nitrogen isotopic values of individual amino acids (AA) in coral host and symbiont tissue has proven to exhibit higher resolution in identifying coral nutrition than bulk analysis. This method allows for distinguishing whether mixotrophic corals obtain their amino acids directly from their symbionts or indirectly via heterotrophic feeding on zooplankton and particulates (Fox et al. 2019, Wall et al. 2021). Compound-specific isotope analysis of amino acids (CSIA-AA) focuses on the isotopic fractionation between individual amino acids brought on by metabolic processes to elucidate biological alterations in an organism's nutrition or metabolism (Ferrier-Pages et al 2021). These assays stem from a disparity between essential and non-essential amino acid accumulation and synthesis. This area of study focuses on thirteen amino acids: Alanine (Ala), Glycine (Gly), Threonine (Thr), Serine (Ser), Valine (Val), Leucine (Leu), Isoleucine (Ile), Proline (Pro), Aspartic acid (Asp), Glutamic acid (Glx), Phenylalanine (Phe), Tyrosine (Tyr), and Lysine (Lys). This study focuses on  $\delta^{13}\text{C}$  values of essential amino acids (EAA) Thr, Val, Leu, Ile, Phe, and Lys. EAA are almost exclusively produced by primary producers and bacteria, requiring most organisms to obtain essential amino acids from diet with minimal isotopic fractionation (Fantle et al. 1999, Reeds 2000, McMahon et al. 2010, 2016). The specific set and isotopic values of

essential amino acids act as an isotopic “fingerprint” that varies between organisms due to differences in metabolic pathways, genetic makeup, and evolutionary factors, such as dietary habits and environmental conditions (Hayes 2001, Larsen et al. 2009, 2013, McMahon et al. 2010, 2016). When applied to corals, this technique is able to trace essential amino acid  $\delta^{13}\text{C}$  “fingerprints” recorded in coral host tissue and determine the proportion of metabolic contribution from either of their autotrophic or heterotrophic sources (Larsen et al. 2009, Fox et al. 2019, Farrier-Pages et al. 2021, Wall et al. 2021). Corals feeding autotrophically are expected to have essential amino acid  $\delta^{13}\text{C}$  fingerprints that overlap with those of symbionts, whereas corals feeding more on heterotrophic sources should show greater overlap with planktonic/particulate endmembers. Using CSIA-AA, Wall et al. (2021) found that *M. capitata* grown under experimental conditions relied entirely on symbionts for their essential amino acids regardless of the mode of feeding (fed/unfed) or duration of the light/dark cycle, indicating autotrophic fidelity rather than trophic plasticity in this coral species. Fox et al. (2018) used CSIA-AA and found that *Pocillopora meandrina* corals in Palmyra exhibit trophic plasticity, exhibiting both autotrophic and heterotrophic feeding at the level of individual colonies on the reef. Thus, highlighting the varied nutritional strategies among coral species, and the ability for CSIA-AA to confidently measure their nutrition.

Amino acid nitrogen isotope analysis ( $\delta^{15}\text{N}_{\text{AA}}$ ) allows for the estimation of the trophic position (TP) of an organism separate from its food source or primary producers (Chikaraishi et al., 2009 & 2014). We can evaluate TP due to the relative difference in  $\delta^{15}\text{N}$  values between *trophic* and *source* amino acids. *Trophic-AAs* (Ala, Asp, Glx, Ile, Leu, Pro, Val) undergo positive enrichment of  $^{15}\text{N}$  relative to the metabolic turnover time of each amino acid whereas *source-AA* (e.g., Lys, Phe, Tyr)  $\delta^{15}\text{N}$  values are conserved through the food web (McClelland and Montoya 2002, Popp et al. 2007). Therefore, the difference between  $\delta^{15}\text{N}$  values of *Trophic-AA* and *Source-AA* allows us to identify the TP of organisms in their respective food webs (McCarthy et al. 2007, Chikaraishi et al. 2009, Fujii et al. 2020). In relation, corals feeding autotrophically had a TP closer to those of primary producers (~1.0) whereas corals feeding heterotrophically exhibited a TP of consumers (~2.0) (Wall et al., 2021, Fujii et al. 2020).

Scleractinian corals and marine macroalgae are in direct competition for habitat and resources on oligotrophic reefs (McCook et al. 2001). Macroalgae can have detrimental effects on corals, such as inhibiting recruitment, growth, and fecundity (Barott et al. 2011 & 2012, Titlyanov et al. 2009, Tanner JE, 1997). Chemically, macroalgae have been proven to produce secondary metabolites (allelochemicals) that have adverse effects on various coral life stages (Titlyanov et al 2009, Gross 2003, Bonaldo and Hay 2014). Donovan et al. (2021) discovered reefs with higher initial macroalgal cover experienced greater coral mortality after bleaching events. A phase shift from a coral-dominated reef to an algal-dominated ecosystem can occur due to environmental change, resulting in a dramatic alteration of the reef's ecological composition and function (Hughes 1994, McCook 1999, Barott et al. 2012). With negative effects exacerbated by local impacts such as overfishing and eutrophication (Birrell et al. 2008, Hoeg-Guldberg 1999).

A new species of “nuisance” red alga, *Chondria tumulosa* was recently documented at Manawai (Pearl and Hermes) and Kuaihelani (Midway) atolls in the Northwestern Hawaiian Islands (NWHI) within the Papahānaumokuākea Marine National Monument (PMNM). The term ‘nuisance’ is used in place of ‘invasive’ due to the lack of knowledge of this alga’s origin. There is a possibility that this alga is a native inhabitant of the atolls and that due to changing oceanic conditions, is acting as an invasive. *C. tumulosa* can form thick (up to 18 cm) mats/mounds overgrowing coral reefs, killing living native corals, algae, and other organisms (Sherwood et al. 2020). Covering several thousand square meters of substrate and exhibiting “tumbleweed” fragmentation, branches can detach from the main growth and inhabit new areas with ocean currents, this alga has the potential to spread and adversely affect other reefs in the PMNM. Since the first documentation at Manawai in 2016, *C. tumulosa* has rapidly spread with increasing abundance in 2019 and 2021 surveys (Sherwood et al. 2020). The confirmation of *C. tumulosa* on Kuaihelani reefs occurred during the 2021 survey with confirmed increased abundance in 2022 (Lopes et al. 2023). These surveys highlight the potential for this alga to further spread across atolls and negatively impact reefs throughout the Hawaiian Island archipelago.

This study aims to understand the physiological changes of coral host and symbionts as influenced by macroalgal cover in the NWHI, using state-of-the-art CSIA-AA. We hypothesized that the presence and abundance of *C. tumulosa* on NWHI reefs would affect the physiology of corals, evident in shifts in their resource assimilation and use, which we infer from changes in bulk tissue and AA carbon and nitrogen isotope values. To investigate this, we designed a sampling plan to collect corals across Manawai and Kuaihelani at varying gradients/abundances of *C. tumulosa* cover, including archived *M. capitata* samples from Manawai collected in 2015, prior to the *C. tumulosa* invasion, along with *Montipora capitata* and a species complex of *Pocillopora meandrina* and *Pocillopora ligulata* (*Pocillopora* spp.) corals from Manawai in 2021 and Kuaihelani in 2022. By filling major knowledge gaps about how potentially harmful algae affect coral species in the NWHI, this study will contribute to conservation efforts aimed at mitigating reef degradation.

## METHODS

### Sample Collection

Coral fragments (ca. 3-6 cm) were collected at Manawai atoll and Kuaihelani atoll in the Papahānaumokuākea Marine National Monument in the Northwestern Hawaiian Islands at depths ranging from 0.61 to 19.5 meters in the Summers of 2015, 2021, and 2022. In 2015, before the discovery of *C. tumulosa*, samples of *Montipora capitata* ( $n = 29$ ) were collected from Manawai. In 2021, coral samples of *Montipora capitata* ( $n = 4$ ), and *Pocillopora* spp. ( $n = 25$ ) were collected from Manawai, and, in 2022, *Pocillopora* spp. corals ( $n = 52$ ) were collected from Kuaihelani. Samples were collected with a hammer and chisel/pruning shears, stored at  $-20^{\circ}\text{C}$  on site, then stored at  $-80^{\circ}\text{C}$  until analysis. Post-invasion (2021, 2022) coral samples were taken alongside *Chondria* reef surveys, with % *C. tumulosa* coverage data ranging from none to high (0-100%) based on visual inspection and estimation of coverage. In addition, we collected environmental metadata (depth, latitude/longitude, benthic type, and reef area) at each site (Table S1). Zooplankton tows were conducted at 6 sites at Kuaihelani using a 30 cm diameter plankton tow (80  $\mu\text{m}$  mesh size) behind a small boat at 5 knots for 10 minutes or until ample material was collected. Contents of the cod end were vacuum filtered onto 80  $\mu\text{m}$  27mm nylon mesh filters and stored at  $-20^{\circ}\text{C}$  on site, then frozen at  $-80^{\circ}\text{C}$  until analysis. Clean *C. tumulosa* samples ( $n = 21$ ) from Manawai and ( $n = 5$ ) from Kuaihelani in 2021 were collected. Each sample was checked for encrusting vertebrates, rinsed with 35% sterile artificial seawater to remove loosely attached epibionts and sand, and vigorously rubbed in distilled  $\text{H}_2\text{O}$  before analysis (Kuba et al., 2021).

### Laboratory Analysis

#### *Bulk tissue stable isotope analysis*

Coral tissues were removed from the skeleton using an airbrush filled with 0.7  $\mu\text{m}$  filtered seawater attached to a compressed air cylinder. The coral slurry (host and symbiont) was briefly homogenized followed by 53  $\mu\text{m}$  nylon mesh filtration to remove skeletal debris (Wall et. al. 2020). Symbiont cells were separated from solution using centrifugation and host cells were decanted from the symbiont pellet. Symbiont pellets were washed with distilled  $\text{H}_2\text{O}$  and frozen for later analysis (Muscatine et al. 1989). The host tissue slurry was then filtered onto pre-burned ( $550^{\circ}\text{C}$ ) 0.7  $\mu\text{m}$  GF/F filters, rinsed with distilled  $\text{H}_2\text{O}$ ,

and frozen. Host filters, symbiont pellets, zooplankton, and *Chondria* samples were lyophilized, pulverized by mortar and pestle (if necessary), weighed to ca. 0.5 mg, and stored at -20°C until analyzed. Isotopic values are reported in delta values ( $\delta$ ) using per mill (‰) notation relative to standard materials: Vienna Pee-Dee Belemnite (V-PDB) and atmospheric N<sub>2</sub> standards (Air) for  $\delta^{13}\text{C}$  and  $\delta^{15}\text{N}$ , respectively. Bulk  $\delta^{13}\text{C}$  and  $\delta^{15}\text{N}$  values and C:N ratios of coral host, symbiont, algae, and plankton tissues were measured using a Costech elemental combustion system coupled to a Thermo-Finnigan Delta Plus XP isotope ratio mass spectrometer on samples packed into tin capsules (Price et. al. 2020).

#### *Individual amino acid isotope analysis*

Approximately 10 mg of coral host, symbiont, *Chondria* algae, and plankton tissues were hydrolyzed, and trifluoroacetyl/isopropyl ester derivatives were created using the methods of Popp et al. (2007) and Hannides et al. (2009). Briefly, samples were hydrolyzed (trace-metal grade 6M HCl, 150°C, 70 min) and the hydrolysate was filtered using low protein-binding filters and purified using cation exchange chromatography. Purified samples were esterified using 4:1 isopropanol:acetyl chloride and derivatized using 3:1 methylene chloride:trifluoroacetyl anhydride. Trifluoroacetyl/isopropyl ester derivatives were also purified using solvent extraction. Samples were prepared with an additional vial containing a mixture of 15 pure AAs purchased commercially (Sigma Scientific). We measured the  $\delta^{13}\text{C}$  values of six AAs considered essential (EAA) for animals—Thr, Val, Leu, Ile, Phe, and Lys—and seven non-essential AAs (NEAA)—Ala, Gly, Ser, Pro, Asp, Glx, and Tyr (Figures S3). Tyr  $\delta^{13}\text{C}$  values were measured but not included in the analysis as it exhibited poor peak shape or coelution with other peaks; Tyr was excluded from data analysis.

$\delta^{13}\text{C}$  values of individual amino acid trifluoroacetyl/isopropyl ester derivatives were determined using an IRMS (MAT 253) interfaced with a Trace GC Ultra via a combustion furnace (1000 °C) and ConFlo IV interface (Thermo Scientific). Samples were injected using a PTV (pressure/temperature/volume) injector, held at 40°C for 3 s, heated to 87°C (400°C min<sup>-1</sup>), heated again to 200 °C and transferred at 200°C using a 1:10 split or splitless for the few samples that were material limited. Helium (1 mL min<sup>-1</sup>) was used as the carrier gas. The gas chromatograph was fitted with a BPX5 *forte* capillary column (30 m x

0.32 mm internal diameter with 1.0  $\mu\text{m}$  film thickness; SGE, Inc.). The oven temperature for the GC started at 40°C and was held for 1 min before heating at 15°C min<sup>-1</sup> to 120°C, then 3°C min<sup>-1</sup> to 190°C, and finally 5°C min<sup>-1</sup> to 300°C where it was held for an additional 10 min. Isotope values are reported in standard  $\delta$ -notation relative to V-PDB. Each sample was analyzed in at least triplicate with a perdeuterated *n*-C<sub>20</sub> alkane with a well-characterized  $\delta^{13}\text{C}$  value co-injected as an internal reference. The 15 AA reference suite was analyzed every three injections, and sample  $\delta^{13}\text{C}$ -AA values were corrected relative to this AA suite following Silfer et al. (1991).

The  $\delta^{15}\text{N}$  values of AA trifluoroacetyl/isopropyl ester derivatives were determined using gas chromatography combustion isotope ratio mass spectrometry (GC-C-IRMS, Hayes et al. 1990). The isotope ratio mass spectrometer (IRMS; Thermo Scientific Delta V) was interfaced to a gas chromatograph (Trace GC and GC-C III Interface; Thermo Scientific) fitted with a 60 m BPX5 *forte* column (0.32 mm internal diameter with 1.0  $\mu\text{m}$  film thickness; SGE, Inc.) through a combustion furnace (980°C), reduction furnace (650°C), and liquid nitrogen cold trap. Helium (1.2 mL min<sup>-1</sup>) was used as the carrier gas. Before analysis, samples were dried and redissolved in an appropriate volume of ethyl acetate. Each sample was analyzed in triplicate when possible, with norleucine and amino adipic acid internal reference compounds co-injected in each run. The suite of 15 pure amino acids was also analyzed every 3 injections to provide an additional measure of instrument accuracy. The  $\delta^{15}\text{N}$  values of all pure amino acid reference compounds were previously determined using the bulk isotope technique described above.

### **Data Analysis**

Bulk  $\delta^{13}\text{C}$  and  $\delta^{15}\text{N}$  values were compared between *M. capitata* and *Pocillopora* spp. host and symbiont fractions to analyze the effect of the independent variable (% *C. tumulosa* cover) and abiotic variables (depth, year) using analysis of covariance (ANCOVA).  $\delta^{13}\text{C}_{\text{H-S}}$  values were calculated for host/symbiont pairs to discern the estimated trophic strategy and used as the basis for choosing samples for CSIA-AA. Percent *C. tumulosa* coverage was binned based on various levels of substrate coverage: Pre-invasion (0%), <1%, 1-20%, 21-70%, and 71-100%. We focused on the carbon isotopic values of essential amino acids as little is known about the isotopic fractionation associated with *de novo* synthesis of non-essential

amino acids for symbiotic cnidarians.  $\delta^{13}\text{C}_{\text{EAA}}$  values were normalized to their respective sample means ( $\delta^{13}\text{C}_N = \text{AA } \delta^{13}\text{C} - \text{sample mean AA } \delta^{13}\text{C}$ ) to reduce spatiotemporal and environmental variability in carbon isotope values at the base of the food web and allow for comparisons across groups. Normalizing  $\delta^{13}\text{C}$  values of AAs to the within-sample mean aligns samples with a common reference point by centering the data around zero (Larsen et al. 2013). Of the 109 coral samples with available bulk host/symbiont isotope values, 11 host (*Montipora capitata*,  $n = 4$ , *Pocillopora* spp.,  $n = 7$ ) and six of their symbionts were chosen for  $\delta^{13}\text{C}_{\text{EAA}}$  analysis alongside zooplankton ( $n = 3$ ) and *C. tumulosa* ( $n = 4$ ) samples. For AA-N analysis, six coral hosts (*Montipora capitata*  $n = 2$ , *Pocillopora* spp.,  $n = 4$ ), three zooplankton, and four *C. tumulosa* samples were analyzed. Due to low sample mass of symbionts associated with *Montipora* and documented similarities in  $\delta^{13}\text{C}_{\text{EAA}}$  values of Symbiodiniaceae (Larsen et al. 2013, Wall et al. 2021, Stahl et al. 2023), symbiont fractions from both holobionts (*Montipora* and *Pocillopora* hosts) were pooled as one endmember in comparative analysis. Similarly, to increase sample size and resolution of heterotrophic sources, we include a pooled zooplankton sample (63–250  $\mu\text{m}$ ) from Kāneʻohe Bay, Oʻahu (Wall et al. 2021), and the average  $\delta^{13}\text{C}_{\text{EAA}}$  values for zooplankton ( $n = 9$ ; > 163  $\mu\text{m}$ ) collected from Palmyra (Fox et al. 2019). Wall et al. showed that planktonic endmembers between Palmyra and Oʻahu had overlapping  $\delta^{13}\text{C}_{\text{EAA}}$  fingerprints that allowed for the addition of literature data into analysis without adding substantial variation. Individual analysis of variance (ANOVA) tests were used to determine the differences in  $\delta^{13}\text{C}$  values for each EAA between groups: *C. tumulosa*, *M. capitata*, *Pocillopora* spp., symbionts, and plankton.

Statistical analysis was performed in *R* (Version 2023.03.0+386). We performed pairwise PERMANOVA (permutational multivariate analysis of variance) to assess differences in multivariate  $\delta^{13}\text{C}_{\text{EAA}}$  values between pairs of sample types. Pairwise comparisons were conducted using the pairwise.adonis function in the pairwiseAdonis package (Martinez Arbizu, 2020). Euclidean distance was used to calculate dissimilarities between samples. Significance was assessed through 999 permutations at  $p < 0.05$ . Principal component analysis (PCA) was used to identify patterns, detect outliers, and visualize relationships between variables. PCA works by condensing high-dimensional data into fewer dimensions, allowing for the interpretation of data. Principal component 1 and 2 were plotted with 95% confidence

interval ellipses, and plots were used to infer trends in the data. We incorporated linear discriminant analysis (LDA) to complement our analytical approach. While PCA primarily captures the variation within the data, LDA focuses on maximizing separation between predefined groups. By integrating LDA alongside PCA, we not only explore the overall structure of the dataset but also gain insights into how well-defined groups are discriminated within the multidimensional space. The data was divided into coral host and their autotrophic symbiont and heterotrophic (plankton and potentially *C. tumulosa*) sources. An LDA was trained in the absence of coral host  $\delta^{13}\text{C}_{\text{EAA}}$  isotope data where source classifications were checked with cross-validation techniques applied to assess model performance. Coral host AA- $\delta^{13}\text{C}$  data was then re-introduced to the model using symbiont, plankton, and *C. tumulosa*  $\delta^{13}\text{C}_{\text{EAA}}$  values as predictors to classify coral host samples as either of the three sources based on their mean-normalized amino acid carbon isotopic composition. Classification accuracy was evaluated by comparing predicted classifications with true labels, and the contribution of individual amino acids to group separation was examined through coefficient analysis.

$$\text{TP}_{\text{Glx/Phe}} = (\delta^{15}\text{N}_{\text{Glx}} - \delta^{15}\text{N}_{\text{Phe}} - b) / \text{TDF} + 1 \quad (\text{Equation 1})$$

$$b = -3.4 \pm 0.9 \text{‰ for aquatic cyanobacteria and algae}$$

$$\text{TDF} = \text{trophic discrimination factor} = 7.6 \pm 1.2 \text{‰}$$

Amino acid-based trophic position ( $\text{TP}_{\text{Glx/Phe}}$ ) was used as a quantitative estimation of where an organism is on the trophic chain using the nitrogen isotopic composition of trophic and source amino acids. Equation 1 describes the basis for this estimation to be made, using a b value of 3.4 and trophic discrimination factor (TDF) of 7.6 for glutamic acid and phenylalanine consistent with ocean food webs (Chikaraishi et al. 2009).

## RESULTS

### Bulk isotopes

Bulk tissue  $\delta^{13}\text{C}$  and  $\delta^{15}\text{N}$  values ranged from -20.9 to -12.0 ‰ and 0.4 to 5.7 ‰, respectively (Fig. 1). In the analysis of covariance (ANCOVA; Table S2), depth ( $p < 0.001$ ) and fraction ( $p < 0.001$ ) significantly influenced  $\delta^{13}\text{C}$  values (Fig. 2). However, genus ( $p = 0.409$ ), year ( $p = 0.261$ ), and the % *C. tumulosa* coverage ( $p = 0.212$ ) were not significant. For  $\delta^{15}\text{N}$  values, fraction, genus, and year ( $p < 0.001$ ) had significant effects, where depth ( $p = 0.575$ ) and *C. tumulosa* abundance ( $p = 0.713$ ) were not significant. Mean host C:N ratios were similar between genera and ranged from 7.5 to 10.7 ‰ for *M. capitata* and 5.7 to 15.9 ‰ for *Pocillopora* spp. Symbiont C:N ratios ranged from 7.2 to 14.8 ‰ for *M. capitata* and 5.6 to 15.1 ‰ for *Pocillopora* spp. related symbionts. Linear analysis showed no difference in C:N ratios between host depth, year, and the interaction between fraction and genus to be significant on C:N ratios. *C. tumulosa* abundance, genus, and host and symbiont fractions did not differ in C:N values ( $p \geq 0.265$ ).

The ANCOVA test on  $\delta^{13}\text{C}_{\text{H-S}}$  values showed *Montipora* did not change with depth or by year sampled ( $p \geq 0.749$ ). Tests showed *Pocillopora*  $\delta^{13}\text{C}_{\text{H-S}}$  values increase significantly with depth ( $p = 0.003$ ) and between sampling years ( $p = 0.002$ ) with the relationship of the two factors also showing significance ( $p = 0.043$ , Fig. 3). Mean  $\delta^{13}\text{C}_{\text{H-S}}$  values between the two genera were similar when combined with the effect of depth ( $p = 0.233$ ).  $\delta^{15}\text{N}_{\text{H-S}}$  values were different between years and across depth ( $p < 0.001$ ) but not different across genera ( $p = 0.066$ , Fig. S1). Analysis of  $\delta^{13}\text{C}_{\text{H-S}}$  and  $\delta^{15}\text{N}_{\text{H-S}}$  values showed the % coverage of *C. tumulosa* did not have an effect on the relative proportion of heterotrophy to autotrophy between years ( $p \geq 0.628$ , Fig. 4, Fig. S2). Corals sampled post-invasion also had no change in  $\delta^{13}\text{C}_{\text{H-S}}$  values associated with % *C. tumulosa* coverage.

### $\delta^{13}\text{C}$ AA analysis

$\delta^{13}\text{C}$  values of thirteen amino acids were extracted from coral host and symbiont tissues, plankton, and *C. tumulosa* (Table S1). For raw values of all thirteen AAs, coral hosts were on average 1.38 ‰ lower than those of the symbionts and the difference in their  $\delta^{13}\text{C}_{\text{AA}}$  values ranged from -3.84 to 1.42 ‰. Both plankton and *C. tumulosa* mean  $\delta^{13}\text{C}_{\text{AA}}$  values were generally lower than the coral fractions in at least

8/13 amino acids. On average across AAs, plankton  $\delta^{13}\text{C}_{\text{AA}}$  values were 0.59, 2.20, and 3.58 ‰ lower than *C. tumulosa*, hosts, and symbiont values respectively. Mean-normalized EAA: Thr, Leu, Ile, and Phe had significantly different  $\delta^{13}\text{C}$  values between groups ( $p \leq 0.047$ ) with Val and Lys showing no distinction ( $p \geq 0.056$ ; Fig. 5, Table S2). Leucine was the most different between tissue types ( $p < 0.001$ ). Mean-normalized  $\delta^{13}\text{C}_{\text{EAA}}$  values are mainly separated by genus ( $p = 0.001$ ) and between years ( $p = 0.017$ ; Table 1). From herein, all references of  $\delta^{13}\text{C}_{\text{EAA}}$  values refer to mean normalized values.

PCA of  $\delta^{13}\text{C}_{\text{EAA}}$  values showed two principal components explained 71.5% of the variance in amino acid values between coral host and symbiont fractions, plankton samples, and *C. tumulosa* samples with 95% confidence (Fig 6). PCA ellipses followed pairwise PERMANOVA results where we observed significant differences in multivariate patterns between our two coral genera, pooled symbionts, plankton, and *C. tumulosa* (Table 2). Endosymbionts, plankton, and *C. tumulosa* were all different from each other ( $p \leq 0.025$ ), representing distinct coral nutritional endmembers. When testing differences of  $\delta^{13}\text{C}_{\text{EAA}}$  fingerprints on genera, host fractions of *Montipora* and *Pocillopora* overlapped ( $p = 0.757$ ). *Montipora* was not different from the symbionts ( $p = 0.204$ ) but different from the plankton ( $p = 0.018$ ). Conversely, *Pocillopora* was marginally different from the symbionts ( $p = 0.078$ ) and not different from the plankton end member ( $p = 0.239$ ). Most notably, all our groups (coral hosts, symbiont algae, plankton) were significantly different from *C. tumulosa* ( $p \leq 0.026$ ).

### **Linear discriminant analysis**

Linear discriminant analysis cross-validations identified nutritional source class membership 60% of the time, with 80% success rates for plankton, but less so for the symbiont (50%) and *C. tumulosa* (50%). Based on the first linear discriminant (LD1), Leu and Phe were the most important EAA for separating the autotrophic and heterotrophic sources whereas Lys and Phe were the primary separators of LD2 (Table S4). The results of the training LDA predictions categorized 3/11 coral samples as the symbiont fraction including two *Montipora* and one *Pocillopora* samples. The remaining 8/11 (two *Montipora* and six *Pocillopora*) samples were categorized as the plankton endmember. None of our coral samples were categorized as the *C. tumulosa* source (Fig 7).

### ***Chondria tumulosa* effect**

The presence (none vs any) and % coverage (binned: none, low, moderate, high) of *C. tumulosa* coverage on reef sampling sites was compared with  $\delta^{13}\text{C}_{\text{EAA}}$  values of coral hosts and their symbionts (Table 3). Comparisons were made to test the effect of *C. tumulosa* on corals sampled before discovery (2015) and after (2021, 2022) to determine if the presence of this alga had a direct effect on coral's physiological uptake of nutrients. Overall, the presence and abundance level of *C. tumulosa* did not affect the  $\delta^{13}\text{C}_{\text{EAA}}$  values of our data.

The % coverage of *C. tumulosa* did not affect *Pocillopora* and *Montipora* host  $\delta^{13}\text{C}_{\text{EAA}}$  values sampled post-discovery ( $p \geq 0.170$ ). Results of PERMANOVAs on  $\delta^{13}\text{C}_{\text{EAA}}$  values indicate the pooled host fractions were marginally indistinct ( $p = 0.067$ ) whereas symbiont fractions were not ( $p = 0.950$ ) across *C. tumulosa* cover bins (Table 3). Additional ANOVA analyses conducted on the  $\delta^{13}\text{C}_{\text{EAA}}$  values in pooled host fractions reveal notable distinctions in Ile, Phe, and Lys among different % coverage bins of *C. tumulosa*. These specific amino acids appear to be the primary contributors to the observed separation (Table 4, Fig 8). *Montipora*  $\delta^{13}\text{C}_{\text{EAA}}$  values were similar between pre- and post-invasion of *C. tumulosa* ( $p = 0.667$ ) and *Pocillopora* showed significant difference in Lys  $\delta^{13}\text{C}_{\text{EAA}}$  values between % coverage bins.

### **$\delta^{15}\text{N}$ AA analysis**

$\delta^{15}\text{N}$  values were analyzed for 12 AAs on samples of *C. tumulosa*, plankton, and host tissue fractions excluding the symbiont ( $n = 13$ ; Figure. 8). Average host  $\delta^{15}\text{N}_{\text{AA}}$  values ranged from -3.45 to 8.65 ‰. *C. tumulosa*  $\delta^{15}\text{N}_{\text{AA}}$  values ranged from -3.97 to 6.26 ‰ and plankton values exhibited the largest range of -7.14 to 11.59 ‰. *C. tumulosa* values were lower than corals and plankton by 2.46 ‰ on average (Table S1). There was high separation between fraction ( $p = 0.001$ ) and genera ( $p = 0.039$ ; Table 1). The pairwise PERMANOVA between paired hosts, plankton, and *C. tumulosa* found variation in  $\delta^{15}\text{N}_{\text{AA}}$  values between all fractions ( $p \leq 0.033$ ; Table S5) and analysis on genera showed distinction in *C. tumulosa* and *Pocillopora* ( $p = 0.034$ ) as well as *C. tumulosa* and plankton ( $p = 0.034$ ). *Montipora* was indistinct from *Pocillopora*, plankton, and *C. tumulosa* ( $p \geq 0.200$ ; Table S6). Trophic  $\delta^{15}\text{N}_{\text{AA}}$  values showed significant

separation between genera (Fig. 9) and the fractionation we observed between source and trophic AA  $\delta^{15}\text{N}$  values allowed for successful quantification of the trophic level of our groups.

### **Amino acid trophic position**

From the difference in AAs Glx and Phe ( $\delta^{15}\text{N}_{\text{Glx}} - \delta^{15}\text{N}_{\text{Phe}}$ ) Trophic position ( $\text{TP}_{\text{Glx-Phe}}$ ) means were calculated for *Montipora*, *Pocillopora*, plankton, and *C. tumulosa*. *Montipora* showed a mean  $\text{TP}_{\text{Glx-Phe}}$  of  $1.09 \pm 0.19$ , *Pocillopora* of  $1.60 \pm 0.37$ , *C. tumulosa* of  $1.53 \pm 0.07$ , and plankton of  $2.34 \pm 0.57$ .

## DISCUSSION

We looked to understand the nutritional strategies of corals as influenced by *C. tumulosa* using state of the art CSIA-AA. We hypothesized that the presence and abundance of *C. tumulosa* on NWHI reefs would impact coral physiology, evident through shifts in resource assimilation and use, which would be reflected in changes in bulk tissue and amino acid carbon and nitrogen isotope values. However, with little evidence to support our hypothesis, we choose to accept the null hypothesis. This study found differences in resource allocation between coral species and colonies, and identified coral and algal isotopic fingerprints to be used to further the study of tropical ecology in the NWHI.

Analysis of bulk tissues revealed differences between host and symbiont  $\delta^{13}\text{C}$  and  $\delta^{15}\text{N}$  values as we investigated the effects of environmental and biological factors on isotopic composition. Furthermore, depth was found to significantly influence  $\delta^{13}\text{C}$  values in both host and symbiont groups, suggesting a previously observed effect of isotope fractionation relative to light attenuation (Wall et al. 2020).  $\delta^{13}\text{C}_{\text{H-S}}$  values were expected to decrease relative to depth supporting the idea of an increase in heterotrophic feeding (or decrease in autotrophic C sharing from symbionts) under lower light. However, with *Montipora* samples only taken at <12m, and *Pocillopora* trending in the opposite direction, this conclusion is not supported by our data. The increase of *Pocillopora*  $\delta^{13}\text{C}_{\text{H-S}}$  with depth could be due to the collection of deeper samples in 2021 relative to 2022 relating to variations in sampling techniques and environmental conditions between years. Perhaps the  $\delta^{13}\text{C}_{\text{H-S}}$  trends that we see regarding heterotrophy/autotrophy are not coupled to light availability with depth in this case, as highly oligotrophic waters in this area allow light to be used more efficiently in photosynthetic processes, thus increasing autotrophy in deeper water. The bulk  $\delta^{13}\text{C}_{\text{H-S}}$  values are subject to higher variability and thus were used as a proxy to choose samples for amino acid compound-specific isotope analysis. We found no effect of % *C. tumulosa* coverage on  $\delta^{13}\text{C}_{\text{H-S}}$  values between sampling years and depths. We have found no evidence that the amount of *C. tumulosa* on a reef is affecting how corals are getting their nutrition and whether they are changing their trophic strategy based on  $\delta^{13}\text{C}_{\text{H-S}}$  values.

CSIA-AA exhibited significant differences in  $\delta^{13}\text{C}$  values with all essential amino acids, except Val and Lys. We tested whether the host and symbiont  $\delta^{13}\text{C}_{\text{EAA}}$  isotopic compositions in *Montipora* and *Pocillopora* were different. While we found there was no difference between  $\delta^{13}\text{C}_{\text{EAA}}$  fingerprints between *Montipora* and *Pocillopora* hosts, our analysis revealed significant differences in how these corals obtain nutrition. The overlap in  $\delta^{13}\text{C}_{\text{EAA}}$  fingerprints between *Montipora* and symbionts confirms the reliance of *M. capitata* on autotrophic nutrition whereas the overlap of  $\delta^{13}\text{C}_{\text{EAA}}$  fingerprints between *Pocillopora* and both the symbiotic and planktonic sources confirms trophic plasticity of *Pocillopora* spp. in concurrence with Wall et al. (2021) and Fox et al. (2019).

A second LDA was constructed using our  $\delta^{13}\text{C}_{\text{EAA}}$  fingerprints alongside *Pocillopora* host ( $n = 14$ ), symbiont ( $n = 11$ ), and plankton ( $n = 9$ ) data from Palmyra (Fox et al. 2019) and *Montipora* host ( $n = 6$ ), symbiont ( $n = 6$ ), and plankton ( $n = 1$ ) data from Kāneʻohe Bay (Wall et al. 2021) data to increase sample sizes of corals and their endmembers. Comparatively, the sources used to train the LDA had a much higher reclassification totaling 88% with 91% for symbionts, 87% for plankton, and 75% for *C. tumulosa*. Based on these new parameters, we again tested to see which of our coral host  $\delta^{13}\text{C}_{\text{EAA}}$  fingerprints overlapped with symbiont, plankton, and *C. tumulosa*. Again, we found that 8/11 of our corals were categorized as the plankton endmember and 3/11 as the symbiont endmember. This second assessment supports the efficacy of this study using LDA and furthers our suggestion of increased resolution into coral nutrition with an increased coral sample size.

We compared our groups with studies that quantify the  $\delta^{13}\text{C}_{\text{EAA}}$  fingerprints of similar tissue types. This allows comparison of the NWHI-specific  $\delta^{13}\text{C}_{\text{EAA}}$  fingerprints of corals, plankton, and algae to datasets from other areas of the Pacific. Coral host  $\delta^{13}\text{C}_{\text{EAA}}$  fingerprints of *Montipora capitata* in Oʻahu and *Pocillopora meandrina* in Palmyra were different than what we quantified (Table 5). We suspect that the tight niche of *M. capitata*  $\delta^{13}\text{C}_{\text{EAA}}$  fingerprints from Kāneʻohe Bay act as a small target for statistical similarities where *M. capitata* in the NWHI showed more variability possibly due to varying nutrient pools between locations and/or differences in their symbiont clade populations which can affect nutrient transfer between the host and their symbionts (Wall et al. 2020). An increase of NWHI *M. capitata* data could be a

solution to observing higher overlap here. *Pocillopora* fingerprint divergence of NWHI and Palmyra data is more expected due to their known trophic plasticity evident in variable EAA fingerprints. NWHI plankton and *M. capitata* symbiont fingerprints were similar compared to those found in O'ahu whereas NWHI plankton and *Pocillopora* symbiont fingerprints were different compared to those of Palmyra. As mentioned, the average  $\delta^{13}\text{C}_{\text{EAA}}$  values of plankton from Palmyra were similar to what we observed in the NWHI.

Comparison of  $\delta^{13}\text{C}_{\text{EAA}}$  fingerprints of plankton with *C. tumulosa* before adding outside data revealed overlaps in fingerprints with no significant differences ( $p = 0.06$ ) between the two groups, suggesting potential interactions such as planktonic grazing on *C. tumulosa* in the NWHI. However, significant differences emerged when considering additional  $\delta^{13}\text{C}_{\text{EAA}}$  fingerprints for plankton from O'ahu (Wall et al. 2021) and Palmyra (Fox et al. 2019). We are justified in pooling these data since there is significant overlap between  $\delta^{13}\text{C}_{\text{EAA}}$  fingerprints of phytoplankton/POM with zooplankton (Fox et al. 2019) and the overlap of O'ahu plankton with plankton from Palmyra (Wall et al. 2021). We further support this assumption with a PERMANOVA of planktonic  $\delta^{13}\text{C}_{\text{EAA}}$  fingerprints between sites ( $p = 0.200$ ).

Like plankton, we compared our *C. tumulosa*  $\delta^{13}\text{C}_{\text{EAA}}$  fingerprints to that of Elliott-Smith et al. (2022) for other Pacific red and green algae. We found separation between red algae and green algae fingerprints supported by the literature. *Chondrus* spp. was the only red algae with statistically similar  $\delta^{13}\text{C}_{\text{EAA}}$  fingerprints to *C. tumulosa* ( $p = 0.200$ ), where other red alga genera: *Plocamium* spp. and *Neorhodomela* spp. were distinct from *C. tumulosa* ( $p = 0.004, 0.032$ ) regardless of apparent overlap within PCA space (Figure S4). It is worth it to note that these red algae we compare *C. tumulosa* to are residents of sites along the coast of the Americas ranging from Alaska to Chile. The sampling of green and red algae from the NWHI to use as a solid comparison to *C. tumulosa* fingerprints we found here would greatly benefit the tropical biogeochemistry field as these studies have yet to be accomplished.

$\delta^{15}\text{N}$  AA analysis of NWHI corals and *C. tumulosa* has confirmed trends of coral nutrition and exposed differences of the nuisance red alga within iso-space. As PERMANOVA analysis held significant

separations between fractions, only mild separation was observed between *C. tumulosa* and both *Pocillopora* and plankton. *Montipora* showed similarity with all groups primarily due to the lack of resolution with only one data point. This study is limited in its ability to draw conclusions based on  $\delta^{15}\text{N}$  AA analysis in the same techniques used for  $\delta^{13}\text{C}$  analysis due to limited data, thus we look to trophic position.

The trophic position ( $\text{TP}_{\text{Glx-Phe}}$ ) of *C. tumulosa* at 1.53 raises questions, as marine primary producers typically exhibit a  $\text{TP}_{\text{Glx-Phe}}$  of about 1.0, however, some red algae analyzed has a  $\text{TP}_{\text{Glx-Phe}}$  of as high as 1.2 (Chikaraishi et al. 2009). This discrepancy may be attributed to processes such as nitrogen remineralization beneath *C. tumulosa* mats from smothered decaying material or sample contamination brought on by metazoans/epiphytes living within the *C. tumulosa* mat. However, sample collection focused on material well above the bottom of the mat and was extensively cleaned of metazoans/epiphytes (H. Spalding, pers comm.). The most likely reason is the presence of Gammaproteobacteria; a heterotrophic bacteria that was found to be associated with *C. tumulosa* (Kuba et al. 2023). Inclusion of heterotrophic bacterial biomass could raise the average  $\text{TP}_{\text{Glx-Phe}}$  of the sample (Jassey et al. 2013, Steffan et al. 2015). Coral  $\text{TP}_{\text{Glx-Phe}}$  values, particularly for *Montipora capitata* at 1.0 and *Pocillopora* spp. at 1.5, support previous research suggesting autotrophic fidelity and mixotrophic capabilities, respectively (Wall et al. 2021, Fox et al. 2019). Plankton  $\text{TP}_{\text{Glx-Phe}}$  values aligned closely with literature findings, indicating consistency in their isotopic niche as primary+ consumers (Hannides et al. 2009).

The presence and abundance of *C. tumulosa* did not have a significant effect on coral bulk,  $\delta^{13}\text{C}_{\text{EAA}}$ , and AA  $\delta^{15}\text{N}$  values between samples. However, linear models comparing mean host  $\delta^{13}\text{C}_{\text{EAA}}$  values exposed variation in Ile, Phe, and Lys between *C. tumulosa* % coverage bins. *C. tumulosa* may affect the  $\delta^{13}\text{C}$  values of individual AAs but we do not have enough evidence to deduce an overall effect on coral nutrition and the potential for compounding factors within our dataset may be the result of this variation.

This study has quantified overlap of both coral genera with autotrophic symbionts combined with the separation of heterotrophic source zooplankton, and nuisance red algae, *Chondria tumulosa*. The separation we see between groups confirms the effectiveness of CSIA-AA as a tool to understand ecological and organismal interactions. The reason for lack of taxonomic delineation of species comes from the misidentification of *Pocillopora* coral species in the NWHI. As the target species was *Pocillopora meandrina*, it has been shown that *Pocillopora ligulata* exhibits a similar morphology and thus common misidentification occurs in the literature (Johnston et al. 2018). We also targeted *Montipora capitata* during the 2022 sampling effort but none were identified during collection across Kuaihelani. We believe this to either be due to extreme cryptic behavior or an extreme decline of this species' abundance due to major bleaching events (Couch et al., 2017). Limitations of this study include variations in environmental conditions, sample collection procedures, and species identification errors, necessitating caution in data interpretation. Future research should focus on increasing AA-CSIA sample sizes, particularly those involving coral, zooplankton, and algal communities, to enhance resolution and provide robust conclusions regarding ecological interactions within coral reef ecosystems.

## CONCLUSION

For the first time, we have quantified the carbon and nitrogen amino acid isotope values of *Montipora* and *Pocillopora* corals as well as plankton and macroalgae *C. tumulosa* in the NWHI representing a significant advancement in the study of tropical coral reef ecosystems. Our study confirmed that there is variation of nutritional strategies between coral species and between coral colonies. The overlap of *Montipora*  $\delta^{13}\text{C}_{\text{EAA}}$  fingerprints with those of their symbiotic endmember as well as the overlap of *Pocillopora* with both the symbiont and plankton fingerprints suggest corals of particular genera assimilate nutrition in ways that are consistent with those in other tropical reef ecosystems. The  $\delta^{13}\text{C}_{\text{EAA}}$  fingerprint overlap is thus supported by  $\delta^{15}\text{N}$   $\text{TP}_{\text{Glx-Phe}}$  outlining the benefit of multiple isotopic assessment within a study. We suggest increasing the number of coral samples processed to have better resolution and backing for trends we begin to see regarding the effect of *C. tumulosa* on the reef. The  $\delta^{13}\text{C}_{\text{EAA}}$  fingerprints of *C. tumulosa* offer valuable insights into the composition of and provide a foundation for future investigations involving this red algal genus. Moreover, they serve as a benchmark for studying the evolutionary dynamics of *C. tumulosa* within marine environments. Interestingly, our findings suggest that the presence of *C. tumulosa* may not directly influence the physiological carbon input of corals in the NWHI. Instead, our observations support that the physical overgrowth of *C. tumulosa* poses a greater threat to coral colonies and reef ecosystems. Additionally, the deviation of zooplankton and *C. tumulosa* amino acid  $\delta^{13}\text{C}$  values away from the comparative Palmyra values towards those associated with *C. tumulosa* in principal component analysis and linear discriminant analysis space implies potential grazing on *C. tumulosa* tissue by zooplankton. However, more sampling and assessment is needed to understand coral-macroalgae interactions and trophic connections. This study underscores the importance of CSIA-AA as a powerful tool for distinguishing intra-ecological groups. Furthermore, it marks the inaugural application of CSIA on corals, algae, and zooplankton in the NWHI, further enriching our understanding of these intricate marine ecosystems.

**Table 1.** Results of PERMANOVA testing effects of tissue fraction†, genus, site, and *C. tumulosa* abundance\* on amino acid carbon and nitrogen isotope values. df indicates the degrees of freedom for the model terms. SS shows the sum of squares for each term. R<sup>2</sup> is the proportion of variance explained by each term. F is the F-statistic for each term. p represents the p-value associated with each term.

<i>AA Isotope Analysis</i>	<i>Effect</i>	<i>df</i>	<i>SS</i>	<i>R</i> <sup>2</sup>	<i>F</i>	<i>p</i>
Mean-Normalized δ <sup>13</sup> C <sub>EAA</sub> values	Fraction†	3	524.61	0.496	9.751	<b>0.001</b>
	Genus	1	12.49	0.012	0.697	0.489
	Site	3	121.00	0.114	2.249	0.058
	Year	1	94.45	0.089	5.267	<b>0.017</b>
	Residual	17	304.86	0.288		
	% <i>Chondria</i> *	4	114.87	0.260	1.492	0.121
	Residual	17	327.19	0.740		
AA δ <sup>15</sup> N values	Fraction†	2	1000.71	0.859	31.542	<b>0.001</b>
	Genus	1	63.24	0.054	3.987	<b>0.039</b>
	Site	1	6.33	0.005	0.399	0.723
	Residual	6	95.18	0.082		
	% <i>Chondria</i> *	2	29.50	0.099	0.221	0.946
	Residual	4	267.36	0.901		

† 'Fraction' compares tissue types: coral host, symbiont, plankton, and *C. tumulosa*.

\* '%*Chondria*' analysis is carried on out on data in the absence of *C. tumulosa* as not to skew comparisons. Significant p-values ( $p < 0.05$ ) are in bold.

**Table 2.** Results of pairwise PERMANOVA testing the effect of tissue fraction interactions on amino acid carbon isotope values.

<i>Tissue comparison</i>	<i>df</i>	<i>SS</i>	<i>R</i> <sup>2</sup>	<i>F</i>	<i>p</i>
<i>Chondria vs Montipora</i>	1	119.567	0.794	23.112	<b>0.026</b>
<i>Chondria vs Pocillopora</i>	1	103.850	0.408	6.212	<b>0.006</b>
<i>Chondria vs Plankton</i>	1	32.708	0.373	4.169	<b>0.025</b>
<i>Chondria vs Symbiont</i>	1	190.075	0.623	13.241	<b>0.004</b>
<i>Montipora vs Pocillopora</i>	1	6.815	0.047	0.439	0.757
<i>Montipora vs Plankton</i>	1	35.153	0.443	5.559	<b>0.018</b>
<i>Montipora vs Symbiont</i>	1	17.389	0.143	1.335	0.204
<i>Pocillopora vs Plankton</i>	1	22.706	0.122	1.387	0.239
<i>Pocillopora vs Symbiont</i>	1	49.151	0.180	2.418	0.078
<i>Plankton vs Symbiont</i>	1	77.477	0.377	5.445	<b>0.006</b>

**Table 3.** PERMANOVA results comparing  $\delta^{13}\text{C}_{\text{EAA}}$  to the % *C. tumulosa* coverage. %*C. tumulosa* coverage binned into none, low, moderate, and high abundance. *Pr>F* represents the p-value associated with each term.

<i>Analysis</i>	<i>Group</i>	<i>df</i>	<i>SS</i>	<i>R</i> <sup>2</sup>	<i>F</i>	<i>Pr&gt;F</i>
$\delta^{13}\text{C}_{\text{EAA}}$	Pooled Host	3	80.426	0.478	2.138	0.080
	<i>Montipora</i>	1	4.934	0.407	1.372	0.667
	<i>Pocillopora</i>	3	95.431	0.658	1.927	0.151
	Post-invasion	3	95.431	0.658	1.927	0.178
	Symbiont	3	35.723	0.327	0.324	0.950
$\delta^{15}\text{N AA}$	Pooled Host	2	26.862	0.377	0.303	0.833
	Plankton	1	52.274	0.715	0.715	0.333

**Table 4.** ANOVA results of individual EAA  $\delta^{13}\text{C}$  values comparing the effect of % *C. tumulosa* on pooled host samples. Results show Ile, Phe, and Lys having mean separation between factor groups.

<i>Amino Acid</i>	<i>term</i>	<i>df</i>	<i>SS</i>	<i>MS</i>	<i>statistic</i>	<i>p</i>
Thr	Bin	3	0.903	0.301	0.096	0.960
Val	Bin	3	9.450	3.150	0.622	0.623
Leu	Bin	3	3.454	1.151	1.786	0.237
Ile	Bin	3	11.681	3.894	5.445	<b>0.030</b>
Phe	Bin	3	8.120	2.707	6.512	<b>0.020</b>
Lys	Bin	3	46.817	15.606	6.091	<b>0.023</b>

**Table 5.** PERMANOVAs of mean-normalized  $\delta^{13}\text{C}_{\text{EAA}}$  values between like tissue types of samples comparing this study's data to previous literature.

<i>Location</i>	<i>Group</i>	<i>df</i>	<i>SS</i>	<i>R</i> <sup>2</sup>	<i>F</i>	<i>Pr&gt;F</i>
Palmyra*	<i>Pocillopora</i>	1	129.350	0.260	6.678	<b>0.001</b>
	Symbiont	2	66.673	0.291	2.467	<b>0.023</b>
	Plankton	1	23.325	0.404	4.749	<b>0.010</b>
O'ahu†	<i>Montipora</i>	1	51.229	0.597	11.833	<b>0.009</b>
	Symbiont	1	23.279	0.526	5.548	0.163
	Plankton	1	11.683	0.466	1.747	0.250

\* Fox et al. (2019). *Functional Ecology*, 33(11), 2203–2214

† Wall et al. (2021). *Limnology and Oceanography*, 64(5), 2011–2028.

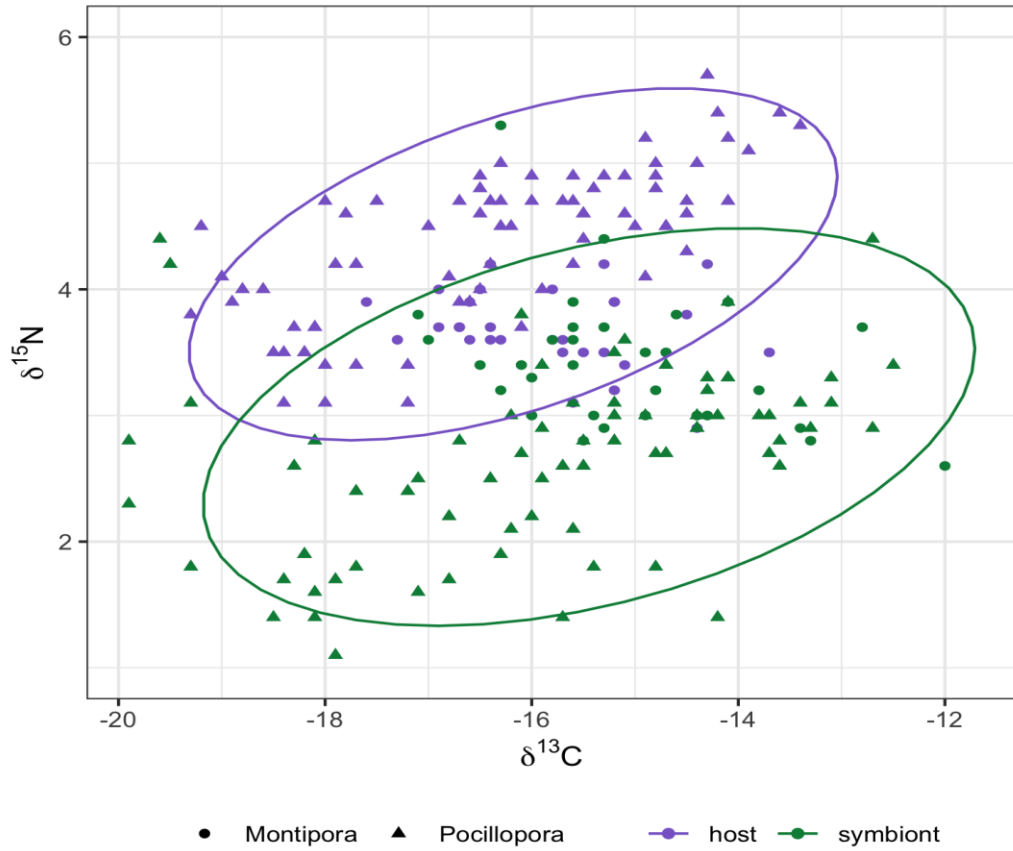


**Fig. 1.** Bulk  $\delta^{13}\text{C}$  and  $\delta^{15}\text{N}$  values of *Montipora* and *Pocillopora* coral host and symbiont tissue. 95% CI ellipses drawn around host and symbiont values to show separation of groups

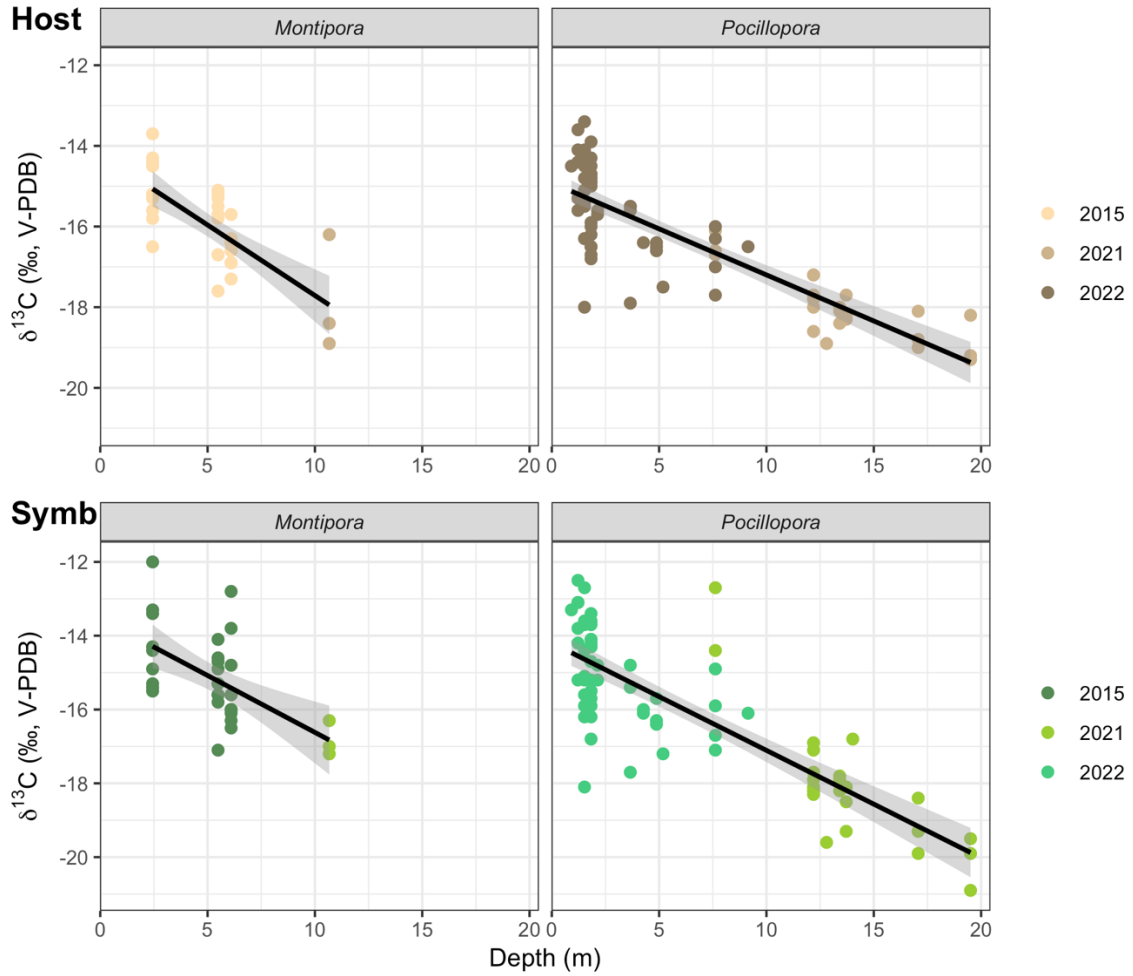


**Fig. 2.** Bulk  $\delta^{13}\text{C}$  values with depth (m) between *Montipora* and *Pocillopora* coral hosts and symbionts. Samples collected in years 2015, 2021, and 2022 are colored accordingly.

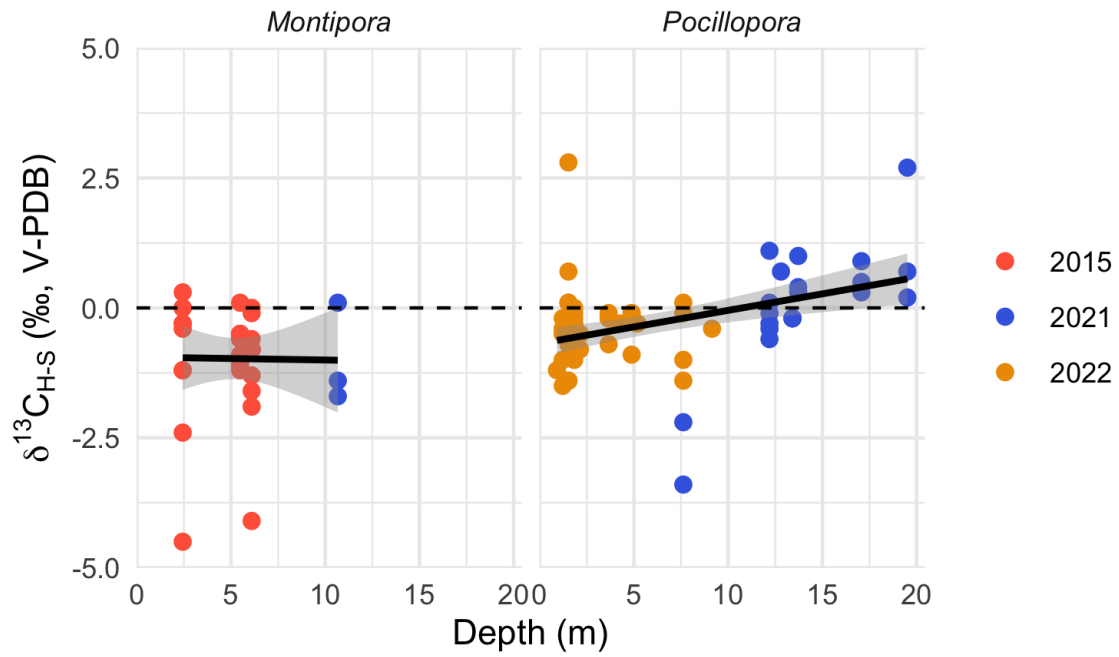


**Fig. 3.** Bulk host  $\delta^{13}\text{C}$  values minus  $\delta^{13}\text{C}$  symbiont values for *Montipora* and *Pocillopora* relative to depth (m) of the colony sampled. Points are colored by sampling year and trendlines are drawn to visualize the relationship between  $\delta^{13}\text{C}_{\text{H-S}}$  values and depth with error included.

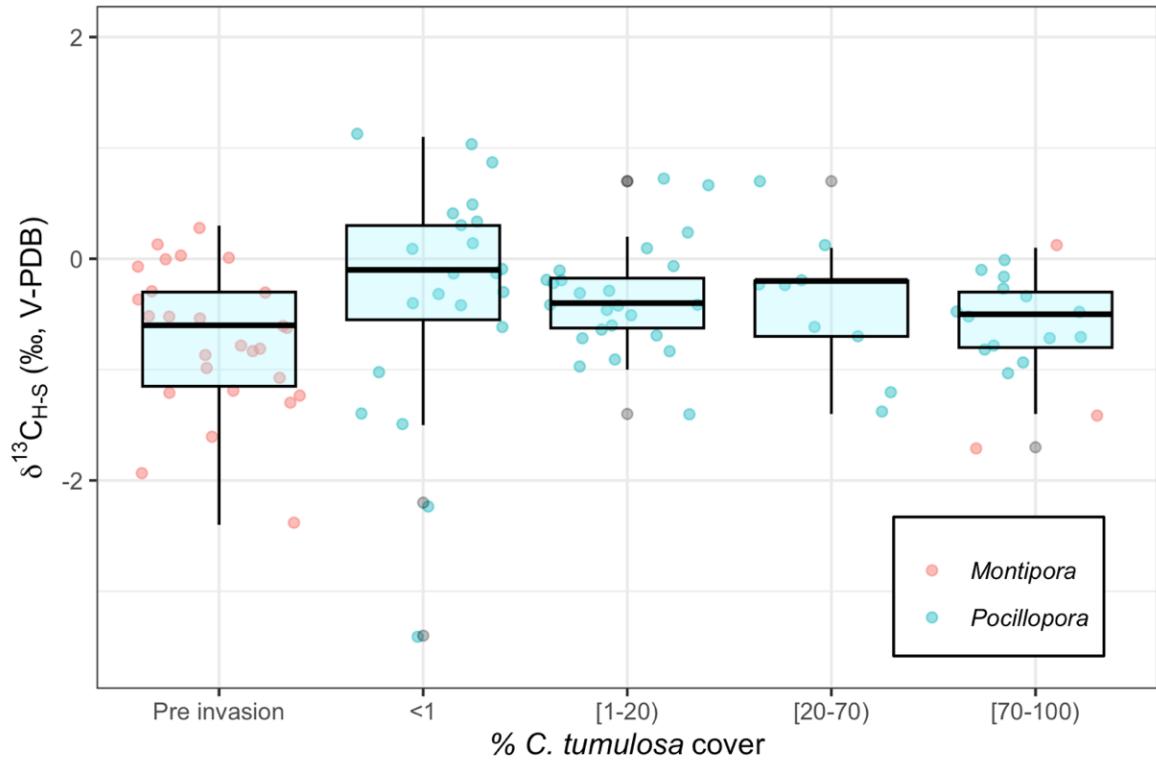


**Fig. 4.** Bulk  $\delta^{13}\text{C}_{\text{H-S}}$  values as a function of varying % *C. tumulosa* cover.

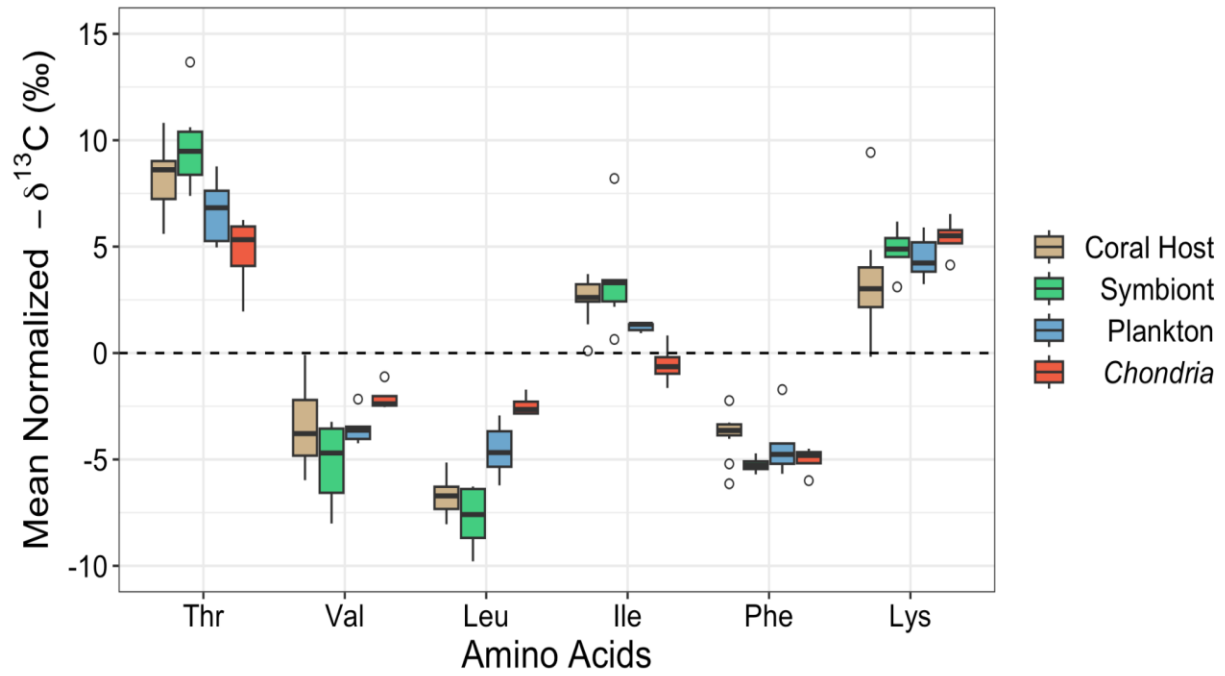


**Fig. 5.**  $\delta^{13}\text{C}$  values of essential amino acids between pooled coral hosts, pooled symbionts, plankton, and *C. tumulosa*. Values listed are mean normalized

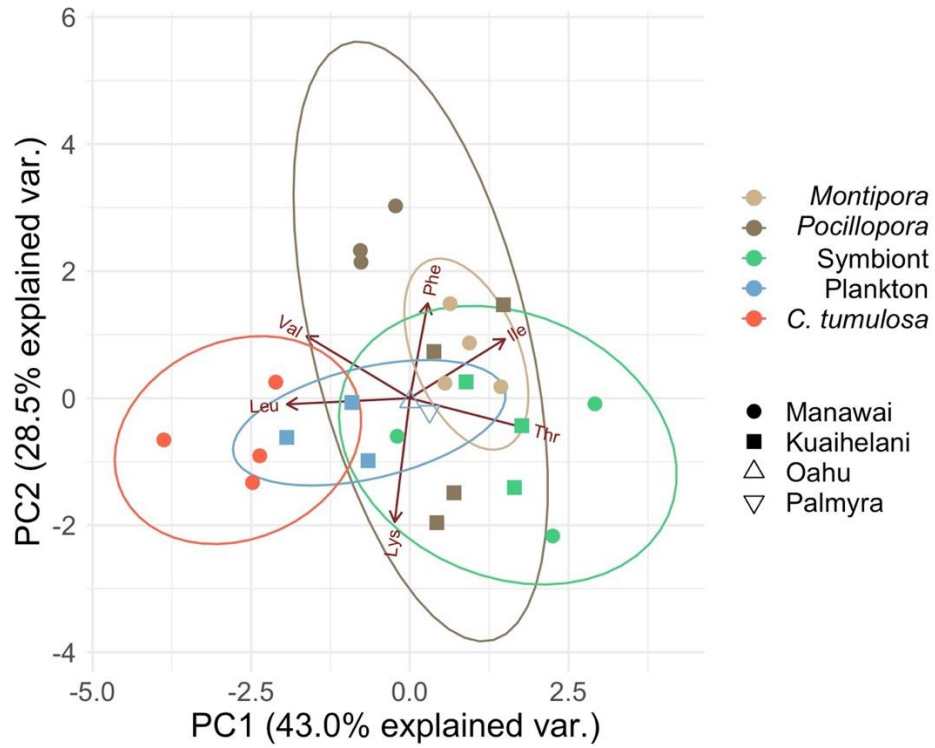


**Fig. 6.** Principal component analysis from  $\delta^{13}\text{C}_{\text{EAA}}$  values of corals: *Montipora capitata* & *Pocillopora* spp., symbionts, plankton, and *C. tumulosa*.

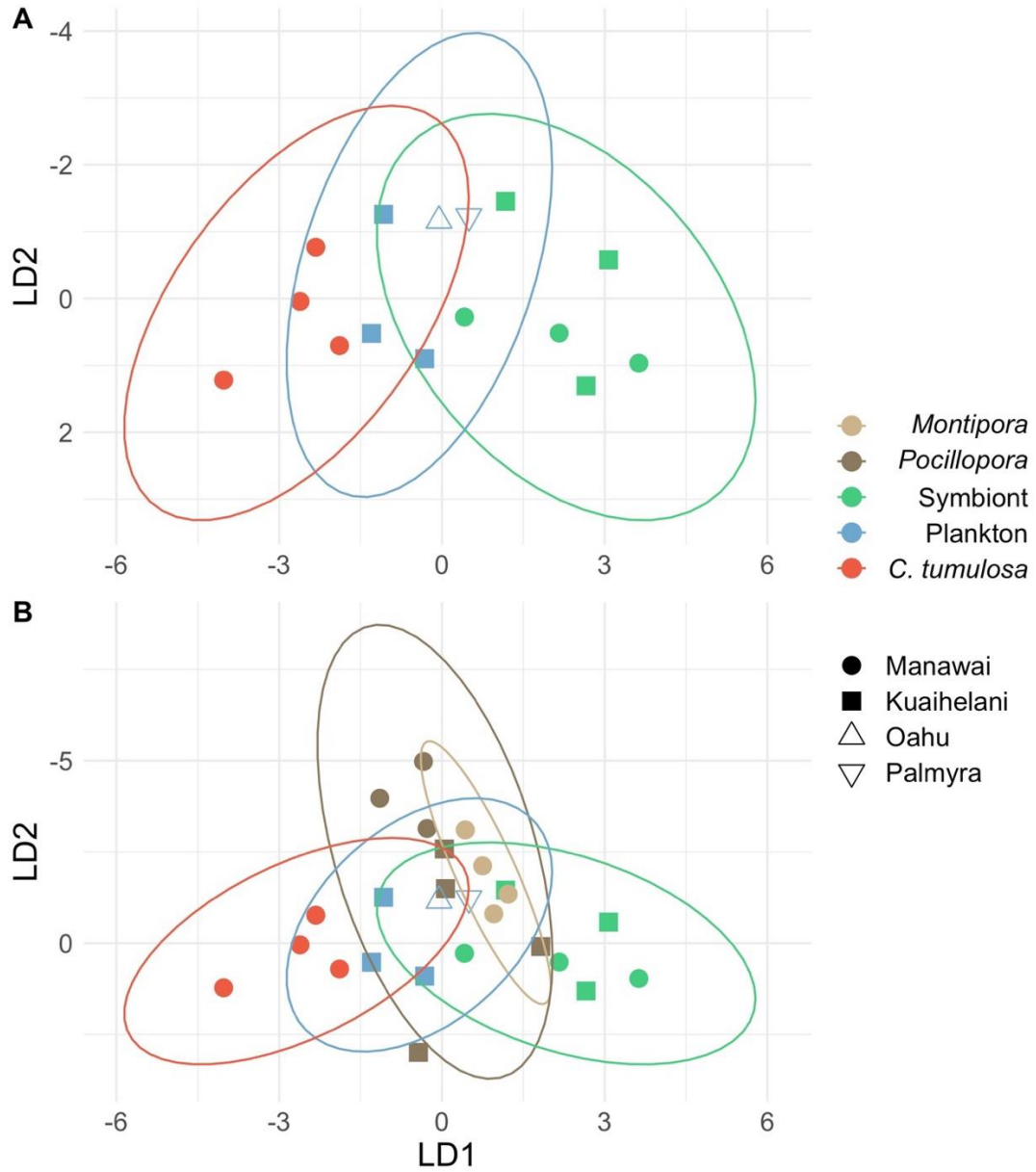


**Fig. 7.** Linear discriminant analysis of  $\delta^{13}\text{C}_{\text{EAA}}$  for *Montipora* (n = 4) and *Pocillopora* (n = 7) corals, symbiont (n = 6) and zooplankton (n = 5) endmembers with *C. tumulosa* (n = 4) included. Lines represent 95% confidence ellipses around each group.

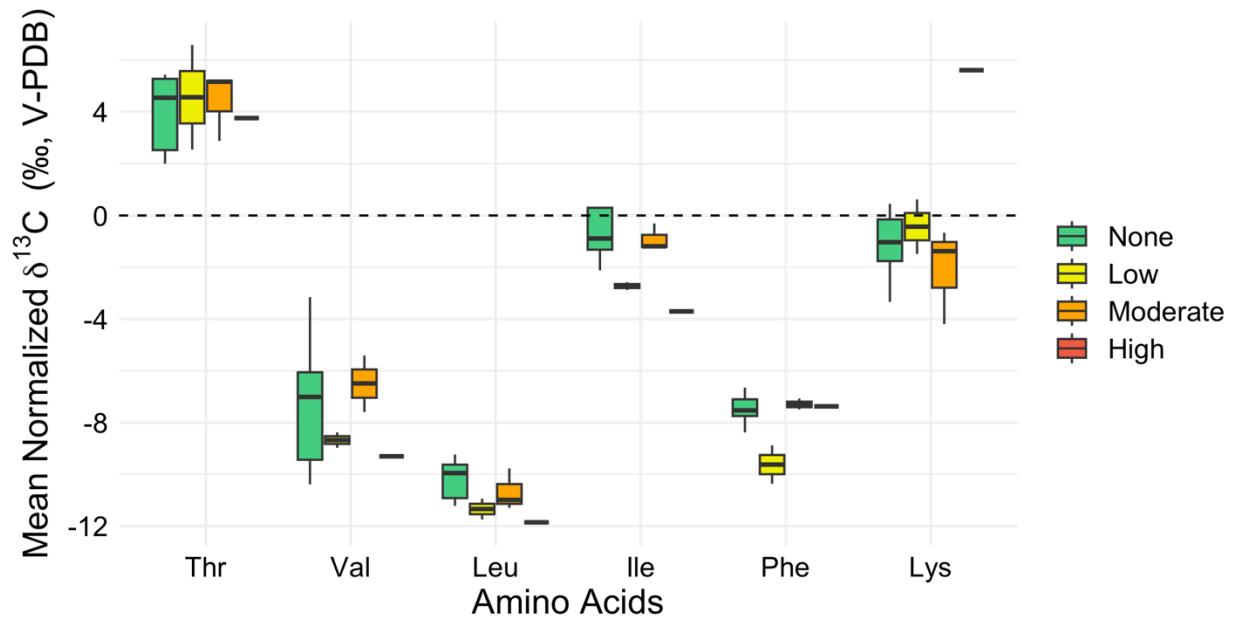


**Fig. 8.** Boxplot of host  $\delta^{13}\text{C}_{\text{EAA}}$  values of each AA. Mean and standard deviation is plotted for host samples taken under various % *C. tumulosa* coverage binned into none, low, moderate, and high. Results of PERMANOVA show significant differences in Ile, Phe, and Lys between binned % cover.

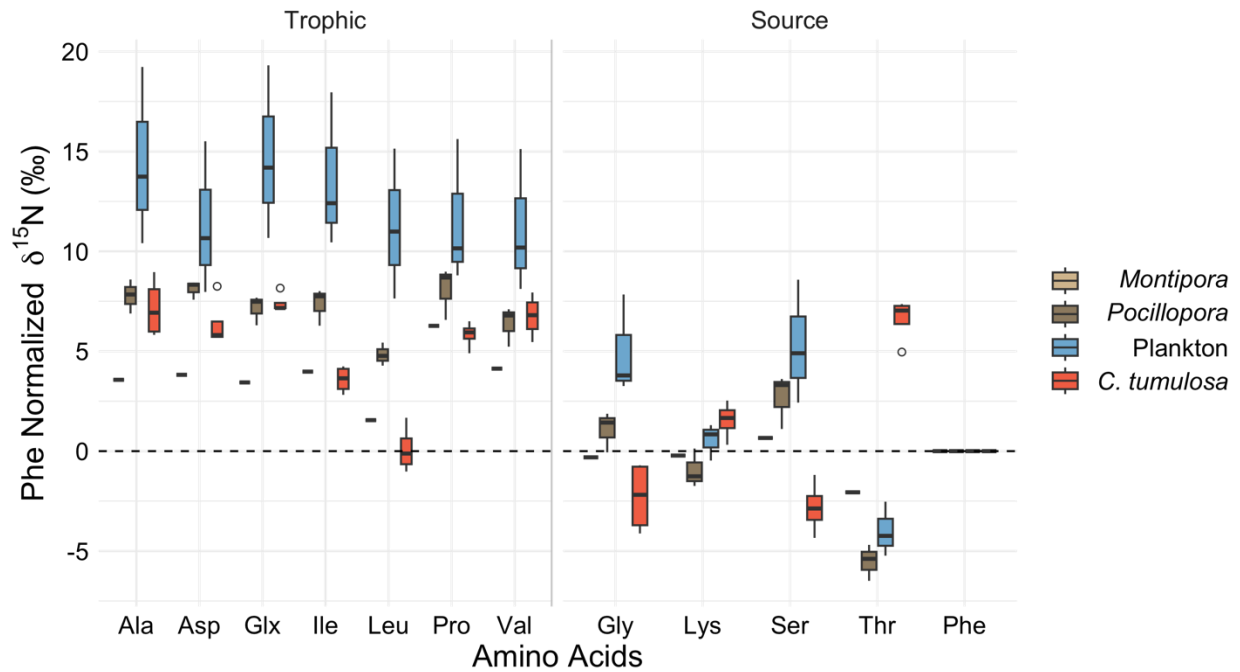


**Fig. 9.**  $\delta^{15}\text{N}_{\text{AA}}$  values of Trophic and Source\* AA for *Montipora* and *Pocillopora* corals, plankton, and *C. tumulosa*. Values are normalized to the  $\delta^{15}\text{N}$  value of Phe in the plot for easy viewing (McClelland and Montoya 2002). \*Gly, Thr, Ser are considered by some to be metabolic AA (McMahon & Newsome, 2019).

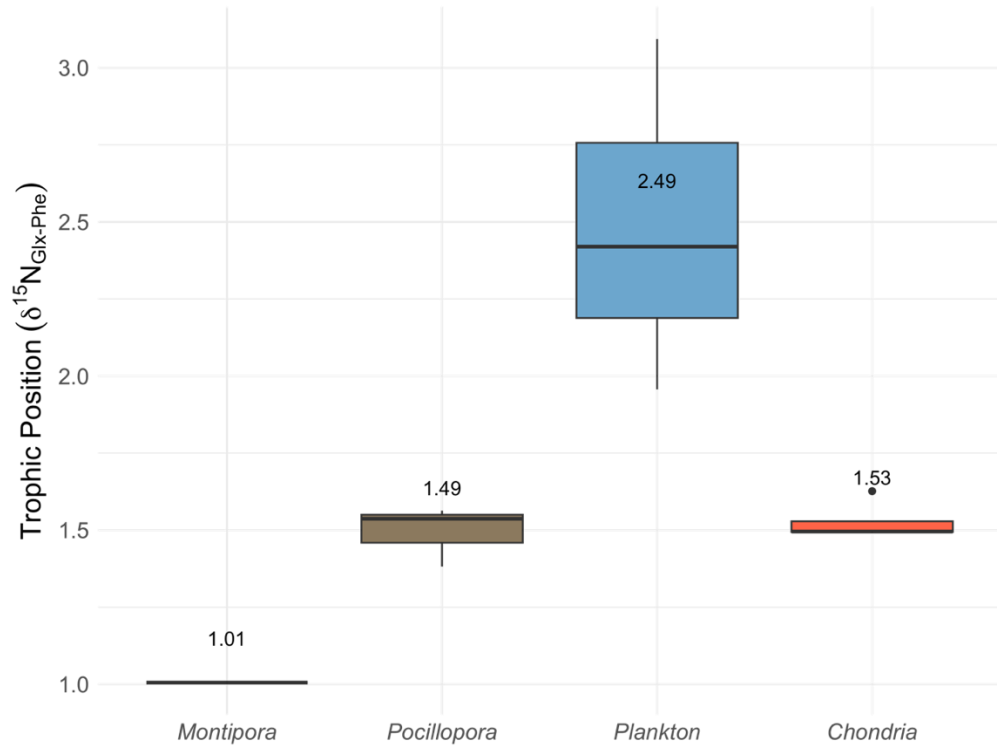


**Fig. 10.** Boxplot of trophic position ( $\text{TP}_{\text{Glx-Phe}}$ ) of groups: *Montipora*, *Pocillopora*, plankton and *C. tumulosa*.

## SUPPLEMENTAL MATERIAL

**Table S1.** Sample collection/analysis metadata link

---

<b>Master datasets available on Zenodo</b>	Kaluhiokalani, M. (2024). Coral-Chondria dataset [Data set]. Zenodo. <a href="https://doi.org/10.5281/zenodo.12193848">https://doi.org/10.5281/zenodo.12193848</a>
--	--

---

**Table S2.** ANOVA tests of mean-normalized essential amino acid  $\delta^{13}\text{C}$  values between coral hosts, symbionts, plankton, and *C. tumulosa*.

Amino Acid	term	df	SS	MS	F-statistic	p value
Thr	Type	3	69.224	23.075	7.470	<b>0.001</b>
Val	Type	3	23.685	7.895	2.936	0.056
Leu	Type	3	82.630	27.543	23.550	<b>0.001</b>
Ile	Type	3	45.482	15.161	7.201	<b>0.002</b>
Phe	Type	3	9.460	3.153	3.110	<b>0.047</b>
Lys	Type	3	17.432	5.811	1.726	0.191

**Table S3.** Individual ANOVA results comparing *Montipora* and *Pocillopora* essential amino acid  $\delta^{13}\text{C}$  values.

<i>Amino Acid</i>	<i>term</i>	<i>df</i>	<i>SS</i>	<i>MS</i>	<i>statistic</i>	<i>p</i>
Thr	Genus	1	3.652	3.652	1.820	0.210
Val	Genus	1	1.566	1.566	0.418	0.534
Leu	Genus	1	0.711	0.711	1.019	0.339
Ile	Genus	1	0.677	0.677	0.599	0.459
Phe	Genus	1	0.134	0.134	0.113	0.744
Lys	Genus	1	0.075	0.075	0.011	0.919

**Table S4.** Results of linear discriminant analysis comparing EAA of genera: *Montipora*, *Pocillopora*, Symbionts, Plankton, and *C. tumulosa*. Leu, Ile, and Thr are the primary drivers separating in LD1 respectively. LD2 is separated by Phe and Lys respectively.

<i>AA</i>	<i>LD1</i>	<i>LD2</i>
Thr	0.192	-0.127
Val	-0.181	-0.230
Leu	<b>-0.432</b>	0.028
Ile	0.222	0.076
Phe	<b>-0.601</b>	<b>-0.458</b>
Lys	-0.137	<b>0.762</b>

**Table S5.** Pairwise PERMANOVAs of  $\delta^{15}\text{N}$  values between fractions.

<i>Comparison</i>	<i>df</i>	<i>SS</i>	<i>F</i>	<i>R2</i>	<i>p</i>
Host vs Alga	1	536.703	35.123	0.854	<b>0.036</b>
Host vs Plankton	1	152.619	5.291	0.514	<b>0.033</b>
Alga vs Plankton	1	806.551	43.092	0.896	<b>0.026</b>

**Table S6.** Pairwise PERMANOVAs of  $\delta^{15}\text{N}$  values between genera.

<i>Comparison</i>	<i>df</i>	<i>SS</i>	<i>F</i>	<i>R</i> <sup>2</sup>	<i>p</i>
<i>Pocillopora</i> vs <i>Montipora</i>	1	63.241	15.955	0.889	0.250
<i>Pocillopora</i> vs <i>Chondria</i>	1	569.125	100.048	0.952	<b>0.034</b>
<i>Pocillopora</i> vs Plankton	1	95.125	4.698	0.540	0.100
<i>Montipora</i> vs <i>Chondria</i>	1	112.544	16.458	0.846	0.200
<i>Montipora</i> vs Plankton	1	171.826	4.703	0.702	0.250
<i>Chondria</i> vs Plankton	1	806.551	43.092	0.896	<b>0.034</b>

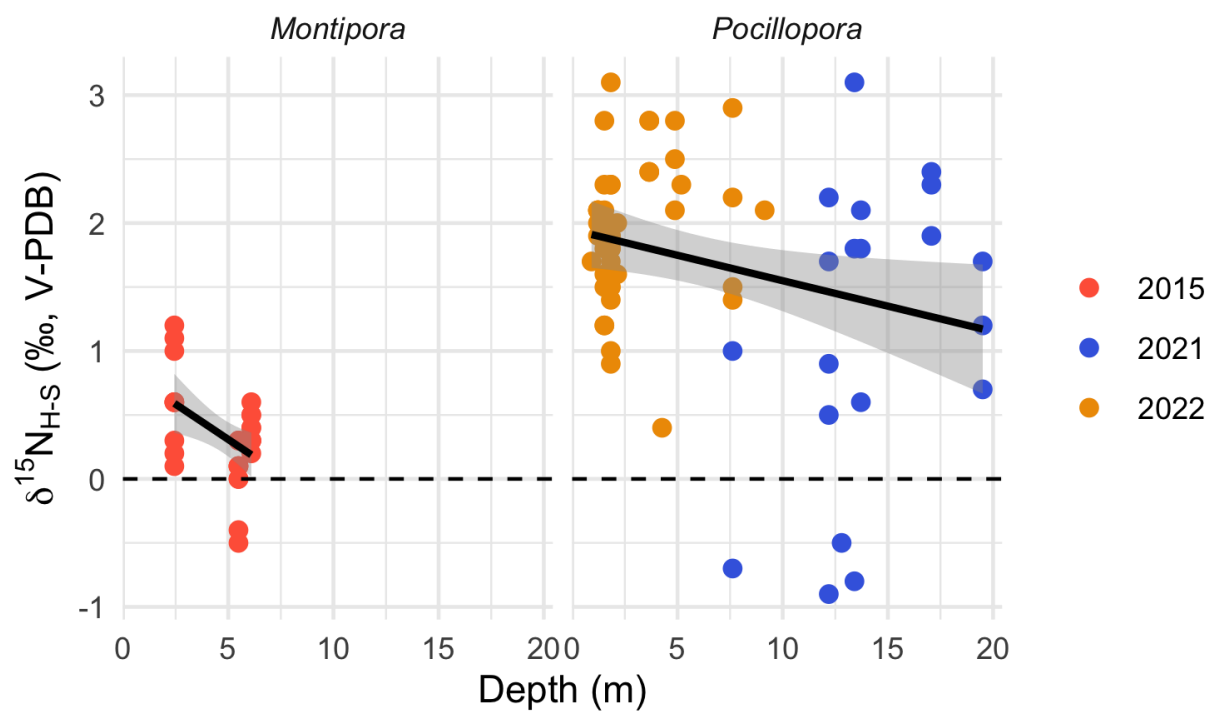


**Fig. S1.**  $\delta^{15}\text{N}_{\text{H-S}}$  values of *M. capitata* and *Pocillopora* spp. corals over a depth gradient between years 2015, 2021, and 2022.

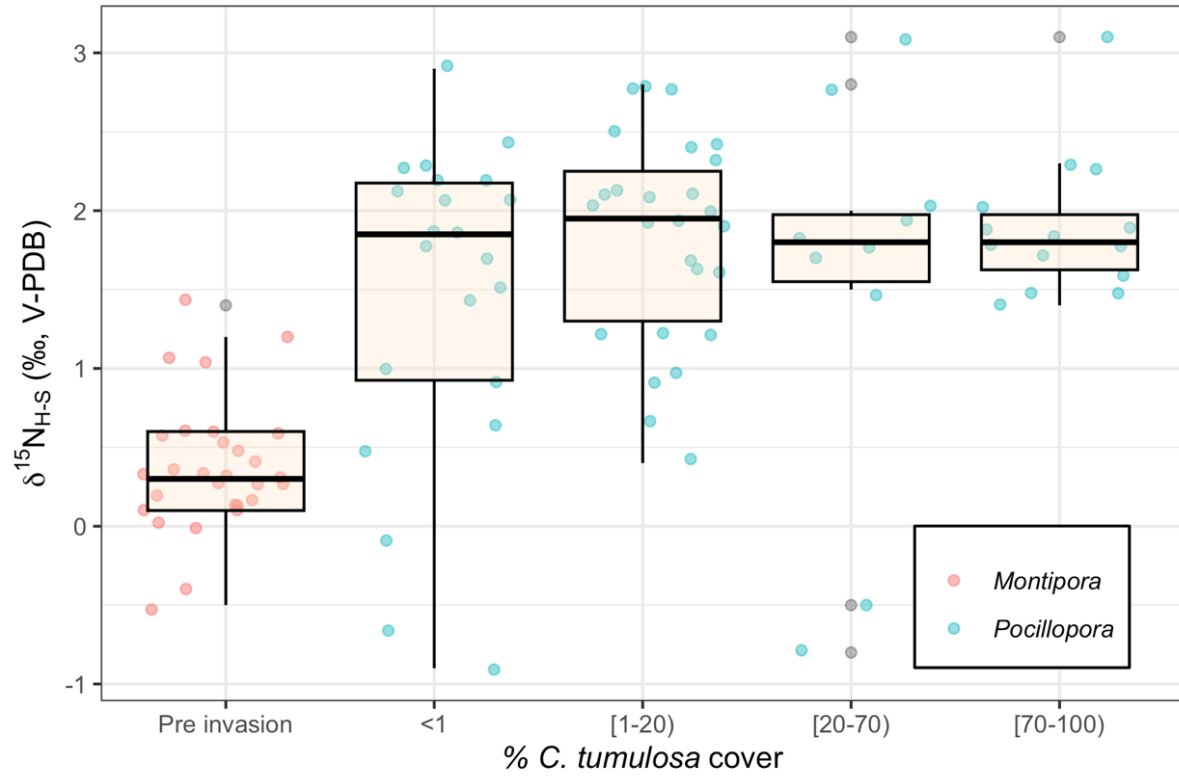


**Fig. S2.** Bulk  $\delta^{15}\text{N}$  host minus symbiont values as a function of varying % *C. tumulosa* cover for *M. capitata* and *Pocillopora* spp. corals.

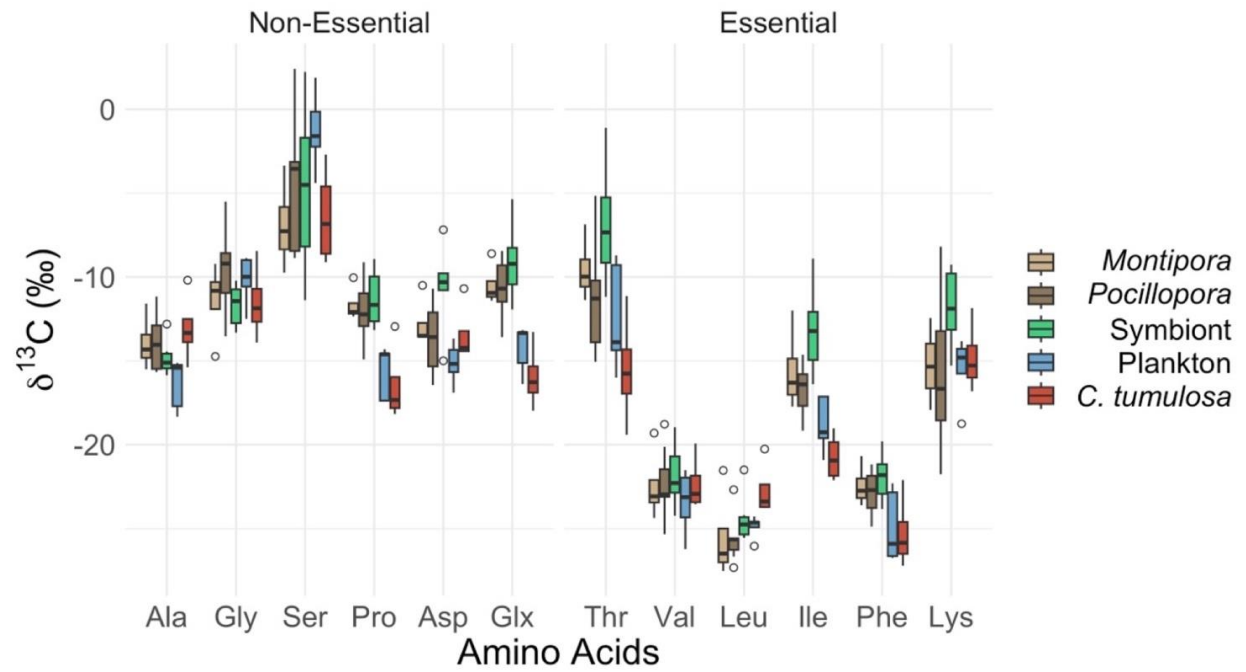


**Fig. S3.** Raw amino acid  $\delta^{13}\text{C}$  values found from CSIA-AA of *M. capitata*, *Pocillopora* spp., pooled symbionts, plankton, and *C. tumulosa*.

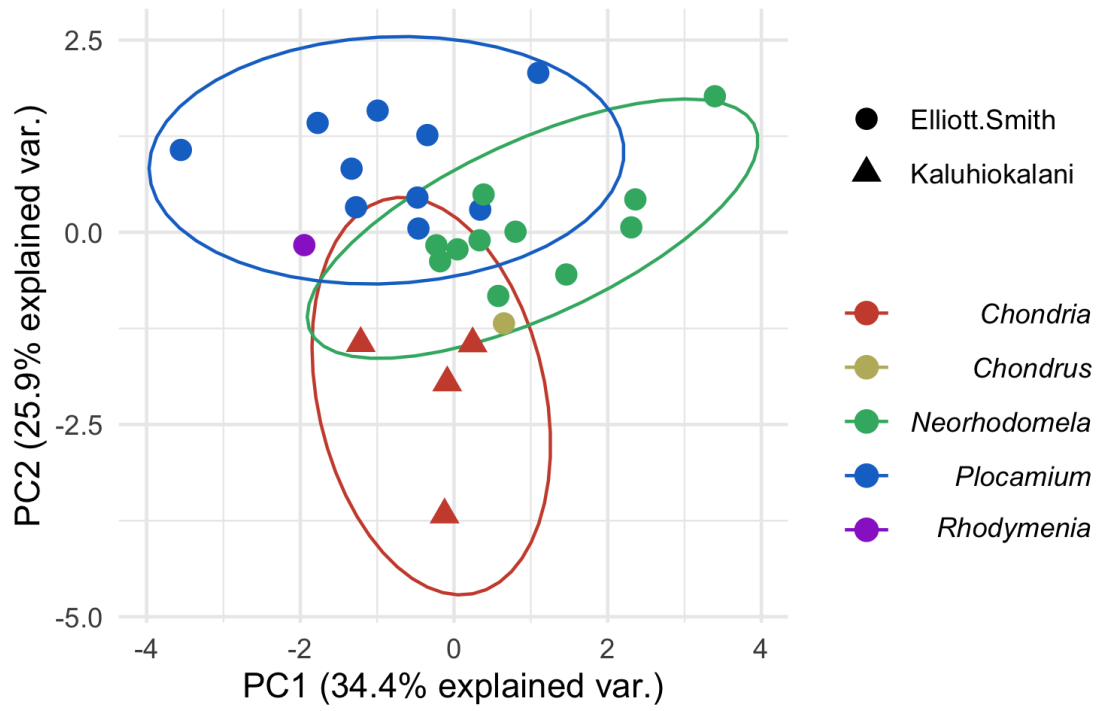


**Fig. S4.** PCA of  $\delta^{13}\text{C}_{\text{EAA}}$  values of *Chondria* compared to other genera of Pacific red algae reported by Elliott Smith (2022).

## REFERENCES CITED

- Aprill, A. (2020). The Role of Symbioses in the Adaptation and Stress Responses of Marine Organisms. *Annual Review of Marine Science*, 12(1), 291–314. <https://doi.org/10.1146/annurev-marine-010419-010641>
- Azam, F., Fenchel, T., Field, J., Gray, J., Meyer-Reil, L., & Thingstad, F. (1983). The Ecological Role of Water-Column Microbes in the Sea. *Marine Ecology Progress Series*, 10, 257–263. <https://doi.org/10.3354/meps010257>
- Baker, A. C., Glynn, P. W., & Riegl, B. (2008). Climate change and coral reef bleaching: An ecological assessment of long-term impacts, recovery trends and future outlook. *Estuarine, Coastal and Shelf Science*, 80(4), 435–471. <https://doi.org/10.1016/j.ecss.2008.09.003>
- Barott, K. L., Rodriguez-Mueller, B., Youle, M., Marhaver, K. L., Vermeij, M. J. A., Smith, J. E., & Rohwer, F. L. (2011). Microbial to reef scale interactions between the reef-building coral *Montastraea annularis* and benthic algae. *Proceedings of the Royal Society B: Biological Sciences*, 279(1733), 1655–1664. <https://doi.org/10.1098/rspb.2011.2155>
- Barott, K., Williams, G., Vermeij, M., Harris, J., Smith, J., Rohwer, F., & Sandin, S. (2012). Natural history of coral–algae competition across a gradient of human activity in the Line Islands. *Marine Ecology Progress Series*, 460, 1–12. <https://doi.org/10.3354/meps09874>
- Besser, A. C., Elliott Smith, E. A., & Newsome, S. D. (2022). Assessing the potential of amino acid  $\delta^{13}\text{C}$  and  $\delta^{15}\text{N}$  analysis in terrestrial and freshwater ecosystems. *Journal of Ecology*, 110(4), 935–950. <https://doi.org/10.1111/1365-2745.13853>
- Birrell, C., LJ, M., Willis, B., & Diaz-Pulido, G. (2008). Effects Of Benthic Algae on The Replenishment of Corals and The Implications for The Resilience of Coral Reefs. In *Oceanography and Marine Biology* (Vol. 46, pp. 25–63). <https://doi.org/10.1201/9781420065756.ch2>
- Boecklen, W. J., Yarnes, C. T., Cook, B. A., & James, A. C. (2011). On the Use of Stable Isotopes in Trophic Ecology. *Annual Review of Ecology, Evolution, and Systematics*, 42(Volume 42, 2011), 411–440. <https://doi.org/10.1146/annurev-ecolsys-102209-144726>
- Bonaldo, R. M., & Hay, M. E. (2014). Seaweed-coral interactions: Variance in seaweed allelopathy, coral susceptibility, and potential effects on coral resilience. *PloS One*, 9(1), e85786. <https://doi.org/10.1371/journal.pone.0085786>

- Burge, C. A., Mark Eakin, C., Friedman, C. S., Froelich, B., Hershberger, P. K., Hofmann, E. E., Petes, L. E., Prager, K. C., Weil, E., Willis, B. L., Ford, S. E., & Harvell, C. D. (2014). Climate Change Influences on Marine Infectious Diseases: Implications for Management and Society. *Annual Review of Marine Science*, 6(1), 249–277. <https://doi.org/10.1146/annurev-marine-010213-135029>
- Chikaraishi, Y., Ogawa, N. O., Kashiyama, Y., Takano, Y., Suga, H., Tomitani, A., Miyashita, H., Kitazato, H., & Ohkouchi, N. (2009). Determination of aquatic food-web structure based on compound-specific nitrogen isotopic composition of amino acids. *Limnology and Oceanography: Methods*, 7(11), 740–750. <https://doi.org/10.4319/lom.2009.7.740>
- Chikaraishi, Y., Steffan, S. A., Ogawa, N. O., Ishikawa, N. F., Sasaki, Y., Tsuchiya, M., & Ohkouchi, N. (2014). High-resolution food webs based on nitrogen isotopic composition of amino acids. *Ecology and Evolution*, 4(12), 2423–2449. <https://doi.org/10.1002/ece3.1103>
- Conti-Jerpe, I. E., Thompson, P. D., Wong, C. W. M., Oliveira, N. L., Duprey, N. N., Moynihan, M. A., & Baker, D. M. (2020). Trophic strategy and bleaching resistance in reef-building corals. *Science Advances*, 6(15), eaaz5443. <https://doi.org/10.1126/sciadv.aaz5443>
- Couch, C. S., Burns, J. H. R., Liu, G., Steward, K., Gutlay, T. N., Kenyon, J., Eakin, C. M., & Kosaki, R. K. (2017). Mass coral bleaching due to unprecedented marine heatwave in Papahānaumokuākea Marine National Monument (Northwestern Hawaiian Islands). *PLOS ONE*, 12(9), e0185121. <https://doi.org/10.1371/journal.pone.0185121>
- Deniro, M. J., & Epstein, S. (1981). Influence of diet on the distribution of nitrogen isotopes in animals. *Geochimica et Cosmochimica Acta*, 45(3), 341–351. [https://doi.org/10.1016/0016-7037\(81\)90244-1](https://doi.org/10.1016/0016-7037(81)90244-1)
- Diaz-Pulido, G., & McCook, L. (2002). The fate of bleached corals: Patterns and dynamics of algal recruitment. *Marine Ecology Progress Series*, 232, 115–128. <https://doi.org/10.3354/meps232115>
- Donovan, M. K., Burkepile, D. E., Kratochwill, C., Shlesinger, T., Sully, S., Oliver, T. A., Hodgson, G., Freiwald, J., & van Woesik, R. (2021). Local conditions magnify coral loss after marine heatwaves. *Science*, 372(6545), 977–980. <https://doi.org/10.1126/science.abd9464>
- Elliott Smith, E. A., Fox, M. D., Fogel, M. L., & Newsome, S. D. (2022). Amino acid  $\delta^{13}\text{C}$  fingerprints of nearshore marine autotrophs are consistent across broad spatiotemporal scales: An intercontinental isotopic dataset and likely biochemical drivers. *Functional Ecology*, 1365-2435.14017. <https://doi.org/10.1111/1365-2435.14017>

- Fantle, M., Dittel, A., Schwalm, S., Epifanio, C., & Fogel, M. (1999). A food web analysis of the juvenile blue crab, *Callinectes sapidus*, using stable isotopes in whole animals and individual amino acids. *Oecologia*, 120, 416–426. <https://doi.org/10.1007/s004420050874>
- Ferrier-Pagès, C., & Leal, M. C. (2019). Stable isotopes as tracers of trophic interactions in marine mutualistic symbioses. *Ecology and Evolution*, 9(1), 723–740. <https://doi.org/10.1002/ece3.4712>
- Ferrier-Pagès, C., Martinez, S., Grover, R., Cybulski, J., Shemesh, E., & Tchernov, D. (2021). Tracing the Trophic Plasticity of the Coral–Dinoflagellate Symbiosis Using Amino Acid Compound-Specific Stable Isotope Analysis. *Microorganisms*, 9(1), Article 1. <https://doi.org/10.3390/microorganisms9010182>
- Fox, M. D., Elliott Smith, E. A., Smith, J. E., & Newsome, S. D. (2019). Trophic plasticity in a common reef-building coral: Insights from  $\delta^{13}\text{C}$  analysis of essential amino acids. *Functional Ecology*, 33(11), 2203–2214. <https://doi.org/10.1111/1365-2435.13441>
- Fox, M. D., Williams, G. J., Johnson, M. D., Radice, V. Z., Zgliczynski, B. J., Kelly, E. L. A., Rohwer, F. L., Sandin, S. A., & Smith, J. E. (2018). Gradients in Primary Production Predict Trophic Strategies of Mixotrophic Corals across Spatial Scales. *Current Biology*, 28(21), 3355–3363.e4. <https://doi.org/10.1016/j.cub.2018.08.057>
- Fujii, T., Tanaka, Y., Maki, K., Saotome, N., Morimoto, N., Watanabe, A., & Miyajima, T. (2020). Organic Carbon and Nitrogen Isoscapes of Reef Corals and Algal Symbionts: Relative Influences of Environmental Gradients and Heterotrophy. *Microorganisms*, 8(8), Article 8. <https://doi.org/10.3390/microorganisms8081221>
- Glynn, P. W. (1984). Widespread Coral Mortality and the 1982–83 El Niño Warming Event. *Environmental Conservation*, 11(2), 133–146. <https://doi.org/10.1017/S0376892900013825>
- Gross, E. M. (2003). Allelopathy of Aquatic Autotrophs. *Critical Reviews in Plant Sciences*, 22(3–4), 313–339. <https://doi.org/10.1080/713610859>
- Grottoli, A. G., Rodrigues, L. J., & Palardy, J. E. (2006). Heterotrophic plasticity and resilience in bleached corals. *Nature*, 440(7088), 1186–1189. <https://doi.org/10.1038/nature04565>
- Hannides, C. C. S., Popp, B. N., Landry, M. R., & Graham, B. S. (2009). Quantification of zooplankton trophic position in the North Pacific Subtropical Gyre using stable nitrogen isotopes. *Limnology and Oceanography*, 54(1), 50–61. <https://doi.org/10.4319/lo.2009.54.1.0050>

- Hayes, J. M. (2001). Fractionation of Carbon and Hydrogen Isotopes in Biosynthetic Processes\*. *Reviews in Mineralogy and Geochemistry*, 43(1), 225–277. <https://doi.org/10.2138/gsrmg.43.1.225>
- Hoegh-Guldberg, O. (1999). Climate change, coral bleaching, and the future of the world's coral reefs. *Marine and Freshwater Research*, 50(8), 839–866. <https://doi.org/10.1071/mf99078>
- Hoegh-Guldberg, O., Skirving, W., Dove, S. G., Spady, B. L., Norrie, A., Geiger, E. F., Liu, G., De La Cour, J. L., & Manzello, D. P. (2023). Coral reefs in peril in a record-breaking year. *Science*, 382(6676), 1238–1240. <https://doi.org/10.1126/science.adk4532>
- Houlbrèque, F., & Ferrier-Pagès, C. (2009). Heterotrophy in tropical scleractinian corals. *Biological Reviews of the Cambridge Philosophical Society*, 84(1), 1–17. <https://doi.org/10.1111/j.1469-185X.2008.00058.x>
- Hughes, T. P. (1994). Catastrophes, Phase Shifts, and Large-Scale Degradation of a Caribbean Coral Reef. *Science*, 265(5178), 1547–1551. <https://doi.org/10.1126/science.265.5178.1547>
- Jassey, V. E. J., Meyer, C., Dupuy, C., Bernard, N., Mitchell, E. A. D., Toussaint, M.-L., Metian, M., Chatelain, A. P., & Gilbert, D. (2013). To What Extent Do Food Preferences Explain the Trophic Position of Heterotrophic and Mixotrophic Microbial Consumers in a Sphagnum Peatland? *Microbial Ecology*, 66(3), 571–580. <https://doi.org/10.1007/s00248-013-0262-8>
- Johnston, E. C., Forsman, Z. H., & Toonen, R. J. (2018). A simple molecular technique for distinguishing species reveals frequent misidentification of Hawaiian corals in the genus *Pocillopora*. *PeerJ*, 6, e4355. <https://doi.org/10.7717/peerj.4355>
- Kaluhiokalani, M. (2024). Coral-Chondria dataset [Data set]. Zenodo. <https://doi.org/10.5281/zenodo.12193848>
- Knowlton, N. (2021). Local management matters for coral reefs. *Science*, 372(6545), 908–909. <https://doi.org/10.1126/science.abi7286>
- Kuba, G. M., Spalding, H. L., Hill-Spanik, K. M., & Fullerton, H. (2021). Microbiota-Macroalgal Relationships at a Hawaiian Intertidal Bench Are Influenced by Macroalgal Phyla and Associated Thallus Complexity. *mSphere*, 6(5), 10.1128/msphere.00665-21. <https://doi.org/10.1128/msphere.00665-21>
- Kuba, G. M., Spalding, H. L., Hill-Spanik, K. M., Williams, T. M., Paiano, M. O., Sherwood, A. R., Hauk, B. B., Kosaki, R. K., & Fullerton, H. (2023). Characterization of macroalgal-associated microbial

- communities from shallow to mesophotic depths at Manawai, Papahānaumokuākea Marine National Monument, Hawai'i. *PeerJ*, 11, e16114. <https://doi.org/10.7717/peerj.16114>
- LaJeunesse, T. C. (2020). Zooxanthellae. *Current Biology*, 30(19), R1110–R1113. <https://doi.org/10.1016/j.cub.2020.03.058>
- Larsen, T., Taylor, D. L., Leigh, M. B., & O'Brien, D. M. (2009). Stable isotope fingerprinting: A novel method for identifying plant, fungal, or bacterial origins of amino acids. *Ecology*, 90(12), 3526–3535. <https://doi.org/10.1890/08-1695.1>
- Larsen, T., Ventura, M., Andersen, N., O'Brien, D. M., Piatkowski, U., & McCarthy, M. D. (2013). Tracing Carbon Sources through Aquatic and Terrestrial Food Webs Using Amino Acid Stable Isotope Fingerprinting. *PLOS ONE*, 8(9), e73441. <https://doi.org/10.1371/journal.pone.0073441>
- Laws, E. A., Bidigare, R. R., & Popp, B. N. (1997). Effect of growth rate and CO<sub>2</sub> concentration on carbon isotopic fractionation by the marine diatom *Phaeodactylum tricornutum*. *Limnology and Oceanography*, 42(7), 1552–1560. <https://doi.org/10.4319/lo.1997.42.7.1552>
- Lesser, M. P., Slattery, M., & Macartney, K. J. (2022). Using Stable Isotope Analyses to Assess the Trophic Ecology of Scleractinian Corals. *Oceans*, 3(4), Article 4. <https://doi.org/10.3390/oceans3040035>
- Levas, S. J., Grottoli, A. G., Hughes, A., Osburn, C. L., & Matsui, Y. (2013). Physiological and Biogeochemical Traits of Bleaching and Recovery in the Mounding Species of Coral *Porites lobata*: Implications for Resilience in Mounding Corals. *PLOS ONE*, 8(5), e63267. <https://doi.org/10.1371/journal.pone.0063267>
- Lopes Jr, K. H., Miura, T., Hauk, B., Kosaki, R., Leonard, J., & Hunter, C. (2023). Rapid expansion of the invasive-like red macroalga, *Chondria tumulosa* (Rhodophyta), on the coral reefs of the Papahānaumokuākea Marine National Monument. *Journal of Phycology*, 59(5), 1107–1111. <https://doi.org/10.1111/jpy.13369>
- Martinez Arbizu, P. (2020). pairwiseAdonis: Pairwise multilevel comparison using adonis. R package version 0.4
- Martinez, S., Kolodny, Y., Shemesh, E., Scucchia, F., Nevo, R., Levin-Zaidman, S., Paltiel, Y., Keren, N., Tchernov, D., & Mass, T. (2020). Energy Sources of the Depth-Generalist Mixotrophic Coral *Stylophora pistillata*. *Frontiers in Marine Science*, 7. <https://www.frontiersin.org/articles/10.3389/fmars.2020.566663>

- McCarthy, M. D., Benner, R., Lee, C., & Fogel, M. L. (2007). Amino acid nitrogen isotopic fractionation patterns as indicators of heterotrophy in plankton, particulate, and dissolved organic matter. *Geochimica et Cosmochimica Acta*, 71(19), 4727–4744. <https://doi.org/10.1016/j.gca.2007.06.061>
- McClelland, J. W., & Montoya, J. P. (2002). Trophic Relationships and the Nitrogen Isotopic Composition of Amino Acids in Plankton. *Ecology*, 83(8), 2173–2180. [https://doi.org/10.1890/0012-9658\(2002\)083\[2173:TRATNI\]2.0.CO;2](https://doi.org/10.1890/0012-9658(2002)083[2173:TRATNI]2.0.CO;2)
- McCook, L. J. (1999). Macroalgae, nutrients and phase shifts on coral reefs: Scientific issues and management consequences for the Great Barrier Reef. *Coral Reefs*, 18(4), 357–367. <https://doi.org/10.1007/s003380050213>
- McCook, L. J. (2001). Competition between corals and algae on coral reefs: A review of evidence and mechanisms. 18.
- McMahon, K. W., Fogel, M. L., Elsdon, T. S., & Thorrold, S. R. (2010). Carbon isotope fractionation of amino acids in fish muscle reflects biosynthesis and isotopic routing from dietary protein. *Journal of Animal Ecology*, 79(5), 1132–1141. <https://doi.org/10.1111/j.1365-2656.2010.01722.x>
- McMahon, K. W., & Newsome, S. D. (2019). Amino Acid Isotope Analysis: A New Frontier in Studies of Animal Migration and Foraging Ecology. *Tracking Animal Migration With Stable Isotopes (Second Edition)*, 173-190. <https://doi.org/10.1016/B978-0-12-814723-8.00007-6>
- McMahon, K. W., Thorrold, S. R., Houghton, L. A., & Berumen, M. L. (2016). Tracing carbon flow through coral reef food webs using a compound-specific stable isotope approach. *Oecologia*, 180(3), 809–821. <https://doi.org/10.1007/s00442-015-3475-3>
- Miller, J., Maragos, J., Brainard, R., Asher, J., Vargas-Angel, B., Kenyon, J., Schroeder, R., Richards, B., Nadon, M., Vroom, P., Hall, A., Keenan, E., Timmers, M., Gove, J., Smith, E., Weiss, J., Lundblad, E., Ferguson, S., Lichowski, F., & Rooney, J. (2008). The State of Coral Reef Ecosystems of the Pacific Remote Island Areas.
- Mills, M. M., & Sebens, K. P. (2004). Ingestion and assimilation of nitrogen from benthic sediments by three species of coral. *Marine Biology*, 145(6), 1097–1106. <https://doi.org/10.1007/s00227-004-1398-3>
- Morris, L. A., Voolstra, C. R., Quigley, K. M., Bourne, D. G., & Bay, L. K. (2019). Nutrient Availability and Metabolism Affect the Stability of Coral–Symbiodiniaceae Symbioses. *Trends in Microbiology*, 27(8), 678–689. <https://doi.org/10.1016/j.tim.2019.03.004>

- Muscatine, L., Falkowski, P. G., Dubinsky, Z., Cook, P. A., & McCloskey, L. R. (1989). The effect of external nutrient resources on the population dynamics of zooxanthellae in a reef coral. *Proceedings of the Royal Society of London. B. Biological Sciences*, 236(1284), 311–324.  
<https://doi.org/10.1098/rspb.1989.0025>
- Muscatine, L., Falkowski, P. G., Dubinsky, Z., Cook, P. A., McCloskey, L. R., & Smith, D. C. (1997). The effect of external nutrient resources on the population dynamics of zooxanthellae in a reef coral. *Proceedings of the Royal Society of London. B. Biological Sciences*, 236(1284), 311–324.  
<https://doi.org/10.1098/rspb.1989.0025>
- Muscatine, L., R. McCloskey, L., & E. Marian, R. (1981). Estimating the daily contribution of carbon from zooxanthellae to coral animal respiration<sup>1</sup>. *Limnology and Oceanography*, 26(4), 601–611.  
<https://doi.org/10.4319/lo.1981.26.4.0601>
- Ohkouchi, N., Chikaraishi, Y., Close, H. G., Fry, B., Larsen, T., Madigan, D. J., McCarthy, M. D., McMahon, K. W., Nagata, T., Naito, Y. I., Ogawa, N. O., Popp, B. N., Steffan, S., Takano, Y., Tayasu, I., Wyatt, A. S. J., Yamaguchi, Y. T., & Yokoyama, Y. (2017). Advances in the application of amino acid nitrogen isotopic analysis in ecological and biogeochemical studies. *Organic Geochemistry*, 113, 150–174. <https://doi.org/10.1016/j.orggeochem.2017.07.009>
- Palardy, J. E., Rodrigues, L. J., & Grottoli, A. G. (2008). The importance of zooplankton to the daily metabolic carbon requirements of healthy and bleached corals at two depths. *Journal of Experimental Marine Biology and Ecology*, 367(2), 180–188. <https://doi.org/10.1016/j.jembe.2008.09.015>
- Palardy, J., Grottoli, A., & Matthews, K. (2005). Effects of upwelling, depth, morphology, and polyp size on feeding in three species of Panamanian corals. *Marine Ecology Progress Series*, 300, 79–89.  
<https://doi.org/10.3354/meps300079>
- Popp, B. N., Graham, B. S., Olson, R. J., Hannides, C. C. S., Lott, M. J., López-Ibarra, G. A., Galván-Magaña, F., & Fry, B. (2007). Insight into the Trophic Ecology of Yellowfin Tuna, *Thunnus albacares*, from Compound-Specific Nitrogen Isotope Analysis of Proteinaceous Amino Acids. In *Terrestrial Ecology* (Vol. 1, pp. 173–190). Elsevier. [https://doi.org/10.1016/S1936-7961\(07\)01012-3](https://doi.org/10.1016/S1936-7961(07)01012-3)
- Post, D. M. (2002). Using Stable Isotopes to Estimate Trophic Position: Models, Methods, and Assumptions. *Ecology*, 83(3), 703–718. [https://doi.org/10.1890/0012-9658\(2002\)083\[0703:USITET\]2.0.CO;2](https://doi.org/10.1890/0012-9658(2002)083[0703:USITET]2.0.CO;2)

- Rädecker, N., Pogoreutz, C., Voolstra, C. R., Wiedenmann, J., & Wild, C. (2015). Nitrogen cycling in corals: The key to understanding holobiont functioning? *Trends in Microbiology*, 23(8), 490–497. <https://doi.org/10.1016/j.tim.2015.03.008>
- Reeds, P. J. (2000). Dispensable and Indispensable Amino Acids for Humans. *The Journal of Nutrition*, 130(7), 1835S-1840S. <https://doi.org/10.1093/jn/130.7.1835S>
- Reynaud, S., Martinez, P., Houlbrèque, F., Billy, I., Allemand, D., & Ferrier-Pagès, C. (2009). Effect of light and feeding on the nitrogen isotopic composition of a zooxanthellate coral: Role of nitrogen recycling. *Marine Ecology Progress Series*, 392, 103–110. <https://doi.org/10.3354/meps08195>
- Rodrigues, L. J., & Grotto, A. G. (2006). Calcification rate and the stable carbon, oxygen, and nitrogen isotopes in the skeleton, host tissue, and zooxanthellae of bleached and recovering Hawaiian corals. *Geochimica et Cosmochimica Acta*, 70(11), 2781–2789. <https://doi.org/10.1016/j.gca.2006.02.014>
- Sherwood, A. R., Huisman, J. M., Paiano, M. O., Williams, T. M., Kosaki, R. K., Smith, C. M., Giuseffi, L., & Spalding, H. L. (2020). Taxonomic determination of the cryptogenic red alga, *Chondria tumulosa* sp. nov., (Rhodomelaceae, Rhodophyta) from Papahānaumokuākea Marine National Monument, Hawai'i, USA: A new species displaying invasive characteristics. *PLOS ONE*, 15(7), e0234358. <https://doi.org/10.1371/journal.pone.0234358>
- Shih, J. L., Selph, K. E., Wall, C. B., Wallsgrove, N. J., Lesser, M. P., & Popp, B. N. (2020). Trophic Ecology of the Tropical Pacific Sponge *Mycale grandis* Inferred from Amino Acid Compound-Specific Isotopic Analyses. *Microbial Ecology*, 79(2), 495–510. <https://doi.org/10.1007/s00248-019-01410-x>
- Silfer, J. A., Engel, M. H., Macko, S. A., & Jumeau, E. J. (1991). Stable carbon isotope analysis of amino acid enantiomers by conventional isotope ratio mass spectrometry and combined gas chromatography/isotope ratio mass spectrometry. *Analytical Chemistry*, 63(4), 370–374. <https://doi.org/10.1021/ac00004a014>
- Stahl, A. R., Ryneerson, T. A., & McMahon, K. W. (2023). Amino acid carbon isotope fingerprints are unique among eukaryotic microalgal taxonomic groups. *Limnology and Oceanography*, 68(6), 1331–1345. <https://doi.org/10.1002/lno.12350>
- Steffan, S. A., Chikaraishi, Y., Currie, C. R., Horn, H., Gaines-Day, H. R., Pauli, J. N., Zalapa, J. E., & Ohkouchi, N. (2015). Microbes are trophic analogs of animals. *Proceedings of the National Academy of Sciences*, 112(49), 15119–15124. <https://doi.org/10.1073/pnas.1508782112>

- Tanner, J. E. (1997). Interspecific competition reduces fitness in scleractinian corals. *Journal of Experimental Marine Biology and Ecology*, 214(1), 19–34. [https://doi.org/10.1016/S0022-0981\(97\)00024-5](https://doi.org/10.1016/S0022-0981(97)00024-5)
- Titlyanov, E. A., Yakovleva, I. M., & Titlyanova, T. V. (2007). Interaction between benthic algae (*Lyngbya bouillonii*, *Dictyota dichotoma*) and scleractinian coral *Porites lutea* in direct contact. *Journal of Experimental Marine Biology and Ecology*, 342(2), 282–291. <https://doi.org/10.1016/j.jembe.2006.11.007>
- Wall, C. B., Kaluhiokalani, M., Popp, B. N., Donahue, M. J., & Gates, R. D. (2020). Divergent symbiont communities determine the physiology and nutrition of a reef coral across a light-availability gradient. *The ISME Journal*, 14(4), 945–958. <https://doi.org/10.1038/s41396-019-0570-1>
- Wall, C. B., Ritson-Williams, R., Popp, B. N., & Gates, R. D. (2019). Spatial variation in the biochemical and isotopic composition of corals during bleaching and recovery. *Limnology and Oceanography*, 64(5), 2011–2028. <https://doi.org/10.1002/lno.11166>
- Wall, C. B., Wallsgrove, N. J., Gates, R. D., & Popp, B. N. (2021). Amino acid  $\delta^{13}\text{C}$  and  $\delta^{15}\text{N}$  analyses reveal distinct species-specific patterns of trophic plasticity in a marine symbiosis. *Limnology and Oceanography*, 66(5), 2033–2050. <https://doi.org/10.1002/lno.11742>
- Wang, J., & Douglas, A. E. (1998). Nitrogen recycling or nitrogen conservation in an alga-invertebrate symbiosis? *The Journal of Experimental Biology*, 201 (Pt 16), 2445–2453. <https://doi.org/10.1242/jeb.201.16.2445>
- Williams, G. J., Sandin, S. A., Zgliczynski, B. J., Fox, M. D., Gove, J. M., Rogers, J. S., Furby, K. A., Hartmann, A. C., Caldwell, Z. R., Price, N. N., & Smith, J. E. (2018). Biophysical drivers of coral trophic depth zonation. *Marine Biology*, 165(4), 60. <https://doi.org/10.1007/s00227-018-3314-2>